FTIR AND POROSITY ANALYSIS OF THE HUMIDITY-EXPOSED PLA-TPU FILAMENTS IN ADDITIVE MANUFACTURING

Submitted in accordance with the requirement of the Universiti Teknikal Malaysia Melaka (UTeM) for the Bachelor Degree of Manufacturing Engineering (Hons.)

by

DORESTEY SINDAM

FACULTY OF MANUFACTURING ENGINEERING

2022

DECLARATION

I hereby, declared this report entitled "FTIR and Porosity Analysis of the Moisture- Exposed PLA-TPU Filaments in Additive Manufacturing" is the results of my own research except as cited in reference.

Signature : .....

Author's Name : DORESTEY SINDAM

Date : 30 JUNE 202

APPROVAL

This report is submitted to the Faculty of Manufacturing Engineering of Universiti Teknikal Malaysia Melaka as a partial fulfillment of the requirements for the degree of Bachelor of Manufacturing Engineering (Hons.). The member of the supervisory committee are as follow:

.....

(DR. RAHIMAH BINTI HJ ABDUL HAMID)

ABSTRAK

Bahagian pencetakan 3D yang biasa digunakan seperti polimer, seperti asid polilaktik (PLA) dan poliuretana termoplastik (TPU), mempunyai kemerosotan bahan yang ketara apabila terdedah kepada kelembapan dan suhu tinggi untuk tempoh yang lama. Berdasarkan itu, penemuan ini menunjukkan bahawa degradasi filamen adalah salah satu kesan utama lembapan dalam filamen disebabkan oleh interaksi antara molekul yang dihasilkan oleh molekul air dengan molekul polimer, dan filamen higroskopik biasanya sensitif untuk menyerap air. Gambaran keseluruhan kajian ini dimulakan dengan perbincangan tentang prinsip percetakan 3D sebelum masuk ke ciri-ciri kritikal percetakan berasaskan polimer dan zarah. Tujuannya adalah untuk mengenal pasti pengaruh air (H_20) pada ikatan rantai kimia polimer filamen PLA-TPU bercetak 3D terdedah kelembapan. Konsep densimeter kemudiannya digunakan untuk menentukan keliangan filamen cetakan 3D (PLA-TPU) terdedah kelembapan di bawah pelbagai keadaan kelembapan dengan menggunakan Prinsip Archimedes. Seterusnya, untuk melihat perubahan struktur filamen cetakan 3D (PLA-TPU) terdedah kelembapan. Analisis spektroskopi inframerah transformasi Fourier (FTIR) bagi percetakan 3D digunakan untuk mencirikan komposisi kimia zarah yang mengandungi zarah mikro dan nano. Selain itu, struktur mikro objek bercetak 3D telah diperiksa menggunakan Mikroskop Elektron Pengimbasan (SEM) dengan salutan sputter yang digunakan supaya imej SEM boleh menjadi kualiti yang diingini. Kajian itu menyimpulkan bahawa kelembapan mengubah rantai kimia ikatan polimer (kumpulan kimia O-H). Selain itu, TPU lebih berliang daripada PLA dan mempunyai ketumpatan yang lebih rendah daripada PLA. Ketumpatan tertinggi dikesan pada PLA, dan ketumpatan terendah ialah TPU, kerana pelbagai keadaan mempengaruhi ketumpatan filamen. Seterusnya, struktur TPU lebih berliang dan lompang di bawah imej SEM daripada struktur PLA. Kajian ini boleh menjadi lebih baik jika tahap kelembapan dikawal oleh peranti seperti kotak kabinet kering dengan kelembapan boleh laras.

ABSTRACT

Commonly used 3D printing parts like polymers, such as polylactic acid (PLA) and thermoplastic polyurethane (TPU), have significant material degradation when exposed to humidity and high temperatures for extended periods. Based on that, these findings show that degradation of the filament is one of the main effects of moisture in a filament due to the intermolecular interactions that the water molecules create with the polymer molecules, and the hygroscopic filaments are usually sensitive to absorbing water. The overview of this study began with a discussion of the principles of 3D printing before going into the critical features of polymer and particle-based printing. The purpose is to identify the influence of water (H_20) on the polymeric chemical chain bonding of the humidity-exposed 3D printed PLA-TPU filaments. The densimeter concepts were then used to determine the porosity of the humidity-exposed 3D printed (PLA-TPU) filaments under various humidity conditions by using the Archimedes Principle. Next, to observe the structural change of humidity-exposed 3D printed (PLA-TPU) filaments. The Fourier transform infrared spectroscopy (FTIR) analysis of 3D printing was used to characterize the chemical composition of particles containing micro and nanoscale particles. Additionally, the microstructure of the 3D printed objects was examined using a Scanning Electron Microscope (SEM) with a used sputter coating so that the SEM images could be of the desired quality. The study concluded that humidity alters the chemical chain of the polymeric bonding (O-H chemical group). Other than that, TPU is more porous than PLA and has a lower density than PLA. The highest density was spotted on PLA, and the lowest density was TPU, because the various conditions were affecting the density of the filament. Next, TPU structural is more porous and void under the SEM image than PLA structural. This study could be better if the humidity level was controlled by a device like a dry cabinet box with adjustable humidity.

DEDICATION

This humble work is dedicated to
my beloved father, Sindam Galakin
my true loved mother, Sianim Ransoi
my adored siblings, and
my appreciated friends
for giving me moral support, cooperation, encouragement,
and understandings. Thank you so much.

ACKNOWLEDGEMENT

First and foremost, praise and thanks to the Almighty for His countless blessings throughout my journey to complete this research work. Without His grace, this final year project could not have become a reality.

I want to express my deep and sincere gratitude to my respected supervisor, Dr. Rahimah Binti Hj. Abdul Hamid, for the great mentoring that was given to me throughout this project. Thank you so much at every point of this research for the precious time, advice, feedback, suggestions, and guidance. It was a great opportunity and a pleasure to work and study under her guidance.

I am highly obliged in taking this opportunity to sincerely thank the head of the JK PSM Committee, En. Nor Akramin bin Mohamad, and all of the assistant engineers for giving me guidance and helping me, as well as providing necessary information regarding this project.

Besides, a special thank you goes to my beloved parents and siblings for their encouragement, support, prayers for the project's success, and financial support. I would like to thank all my friends, especially my classmates and roommates, for their unlimited support and for giving me much motivation and cooperation in completing this report.

Finally, my appreciation goes to those who have helped me directly and indirectly in completing this report. I am very thankful that many people have supported and inspired me to carry out this project, as well as expressing my apology that I could not personally mention each one of you.

TABLE OF CONTENTS

LIST OF TABLES

LIST OF FIGURES

LIST OF ABBREVIATIONS

3D	-	Three dimensional
ABS	-	Acrylonitrile butadiene styrene
AM	-	Additive manufacturing
ASTM	-	American society for testing and materials
CAM	-	Computer Aided-Design
DMA	-	Dynamic mechanical analysis
FDM	-	Fused Deposition Modelling
FTIR	-	Fourier transform infrared
HIPS	-	High-intensity polystyrene
ISO	-	International Organization for Standardization
Mw	-	Molecular weight
N-H	-	Nitrogen-Hydrogen
PDLA	-	Poly (D-lactic acid)
PDLLA	-	Amorphous poly (D, L-lactic acid)
PE	-	Percentage of error
PEEK	-	Polyether ether ketone
PEI	-	Polyetherimide
PET	-	Polyethylene terephthalate
PETG	-	Polyethylene terephthalate glycol
PLA	-	Polylactic acid
PLLA	-	Poly (L-lactic acid)
Pt	-	Platinum
ROP	-	Ring opening polymerization RP - Rapid prototyping
SEM	-	Scanning electron microscope
SOP	-	Standard operation procedure

SLA	-	Stereolithography
STL	-	Standard triangle language
Tg	-	Glass transition temperature
THF	-	Tetrahydrofuran
Tm	-	Melting temperature
TPU	-	Thermoplastic polyurethane

LIST OF EQUATIONS

LIST OF SYMBOLS

Cm	-	Centimetre
m	-	Metre
%	-	Percent
g/cm^3	-	Grams per centimetre cube
g/m3	-	Gram per metre cube
g/ml	-	Gram per millilitre
g/mol	-	Gram per molecule
J/g	-	Joule per gram
mm	-	Millimetre
MPa	-	Mega Pascal
GPa	-	Giga Pascal
°C	-	Degree Celsius
TPa	-	Tera Pascal
W/mK	-	Watt per metre per Kelvin
K	-	Kelvin
nm	-	Nanometre
kg.cm3	-	Kilogram centimetre cube
phr	-	Part per hundred resin
τ_{ISS}	-	Interfacial shear strength
P	-	Peak force
kg	-	Kilograms

mm/min.	-	Millimetre per minute
mm/s	-	Millimetre per second
N	-	Newton
N/mm2	-	Newton per millimetre square
nm	-	Nano metre
kN	-	Kilo newton
W	-	Sample width
B	-	Sample thickness
K_{IC}	-	Fracture toughness
W_m	-	Matrix mass
W_f	-	Fibre mass
m	-	Mass
v	-	Volume
p_f	-	Kenaf density
p_m	-	Matrix density
°C/min	-	Degree celsius per minute
μm	-	Micron metre

CHAPTER 1

INTRODUCTION

This chapter describes the introduction of this research work, including the background, problem statement, objective, scope, and significance of the study. In this work, the analysis of the Fourier-transform infrared spectroscopy (FTIR) and porosity of the moisture-exposed PLA and TPU filaments are carried out.

1.1 Background of Study

3D Printing, often known as Additive Manufacturing (AM), is a contemporary manufacturing process that has grown in popularity. Physical models and complicated geometric constructions may be generated with great precision and at a reasonable cost using 3D printing. The military and other businesses have widely used customizable and uncomplicated 3D printing because of its ability to produce working models and conceptual models and prototypes in a short period (Liao et al., 2019).

According to Amza et al. (2021), Fused Deposition Modelling (FDM) is one of the most often utilized AM techniques because of its ease of use, flexibility, and low-cost technology that employs thermoplastic polymers with hot melt adhesive properties. The FDM technology creates three-dimensional (3D) structures by layering the primary material through the heated nozzle of the FDM 3D printer.

One of the most common raw materials for Polylactic Acid (PLA) plastic is maize starch, and it is commonly used in the production of the product. Typically, the monomer is produced from fermented plant starch. It is a thermoplastic aliphatic polyester utilized as the principal natural raw material in 3D printing.

PLA is an entirely biodegradable thermoplastic polymer made from renewable essential ingredients and is one of the most common 3D printing materials in the market today. TPU, or thermoplastic polyurethane, is the thermoplastic elastomer, a mix of rubber and plastic. PLA is a popular feedstock for desktop Fused Filament Fabrication (FFF) 3D printers. According to Wang et al. (2018), PLA is popular for 3D printing because it is easy to sand, paint, or post-process. As a result, the FDM 3D printer may create a solid product after the semi-liquid extrusion of the source material. TPU is a robust, flexible, durable polymer resistant to abrasions such as oils and lubricants. Because of its unique rubber-plastic blend, it is appropriate for a wide range of applications, including automotive, sports, and textile coatings, as well as breathable films. There are numerous other uses for thermoplastic polyurethane (TPU), including instrument panels for vehicles, wheels for sporting goods, medical equipment, drive belts, shoes for inflatable rafts, and a wide range of extruded film, sheet, and profile applications. TPU is also used in a wide range of other products. TPU is a highly recyclable and biodegradable material (Li and Huneault, 2011).

Humidity is one of the key factors influencing the filament's properties. If the PLA and TPU filaments are subjected to heavy moisture for an extended period, the filament has lost tensile strength at printing, allowing bubbles to emerge on the product's surface (Valerga et al., 2018). Furthermore, PLA and TPU are humidity sensitive, and exposure to excessive moisture causes changes in their characteristics. According to Mitchell et al. (2015), the elongation ratio, degradation rate, and average molecular weight increase when humidity increases. As a result, the mechanical properties of the 3D printed parts will decrease due to the changes in the chemical structure of the polymer with the exposure to water (H_2O). Therefore, in this study, the influence of humidity on the chemical bonding of two different thermoplastic polymers (PLA, TPU) was investigated through Fourier-transform infrared spectroscopy (FTIR) analysis. In addition, the porosity of the 3D printed parts exposed to various humidity conditions was examined through the densimeter by using the Archimedes Principle. Finally, the microstructure was analyzed using a Scanning Electron Microscope (SEM) machine.

1.2 Problem Statements

Humidity refers to the amount of moisture or water in the air, which has become a nemesis for 3D printing users who have embraced the FDM technology due to thermoplastic polymers. When stored in a humid environment, the polymeric filament absorbs moisture or humidity. Moisture saturation occurs after prolonged exposure to even mildly damp indoor air. PLA is an organic substance that quickly absorbs moisture and is particularly sensitive to trace water levels (Zaldivar et al., 2018). As a result, humidity and ultraviolet (UV) radiation can increase the breakdown of the filament, weakening it and causing prints to be inconsistent or of low quality. When the filament absorbs water, and the 3D printer heats it for extrusion, the water and heat combine to form steam, which causes the filament to bubble as it exits the hot end, resulting in an uneven surface on the print. When there is a large concentration of water vapor in the air, the humidity level will be elevated. According to Hossain et al. (2014), water altered the polymeric chain bonding of the printed material while also affecting the mechanical properties. Manufacturing effective 3D printed goods necessitate a thorough grasp of the mechanical characteristics of 3D printed components. Mechanical qualities of 3D printed objects typically differ from conventionally manufactured parts. Excessive humidity can cause the PLA and TPU filaments to degrade (Elmrabet and Siegkas, 2020).

Humidity influences the chemical bonding of the PLA and TPU polymer chains in 3D printed parts. As a result, a chemical analysis of the moisture-exposed filament is significant to ascertain the chemical bonding modifications between the humidity-exposed and original filaments (Shahmirzadi et al., 2021). Additionally, moisture may influence the porosity of the 3D-printed parts due to the inconsistent layer bonding mechanism resulted from poor material extrusion, in addition to the bubbles formation during printing. Therefore, a FTIR and porosity analysis are substanstial as FTIR spectroscopy is used to determine the amount of infrared (IR) radiation absorbed by a Micro Plastic (MP) sample, enabling the study of its molecular composition. An infrared spectrum is a material fingerprint, with absorption peaks matching the vibrational frequencies of the atoms' bonds. Since each polymer material comprises a unique combination of particles, no two compounds have the same infrared spectrum. Thus, FTIR can be used to determine the chemical composition of a polymer molecule (Nodari and Ricciardi, 2019). The filament was subjected to varying humidity

levels to achieve a range of moisture concentrations.

On the other hand, moisture also influences the filament's diameter during storage. After 150 hours of operation under standard conditions, PLA filament may expand up to 40 micrometres before saturation. As a result, 3D printers rely on close tolerances and extremely thin layer heights. Additionally, the TPU elastomer is slightly hygroscopic, collecting moisture from the surrounding air. Assume that the filament becomes excessively saturated with water in an overly humid environment, like one near the seaside. In that instance, print quality difficulties such as air pockets may occur. However, no comparative study has been conducted to educate 3D printer users about the need to seal old filament in an airtight container with desiccant gels as an alternative to dry cabinets. So, it's important to do a study that looks at how humidity affects different thermoplastics.

1.3 Objectives of Study

The objectives of this study are as follows:

i. To identify the influence of water absorption (H_2O) in the polymeric chemical chain bonding of the humidity-exposed 3D printed PLA-TPU filaments using Fourier Transform Infrared Spectroscopy (FTIR).

ii. To measure the porosity of the humidity-exposed 3D printed PLA-TPU filaments restructured under different humidity conditions using a densimeter (Archimedes Principle).

iii. To observe the structural changes of the humidity-exposed 3D printed PLA-TPU filaments through microstructure analysis using a Scanning Electron Microscope (SEM) machine.

1.2 Scopes of Study

The scope of this study are as follows:

a) A red PLA and TPU filaments with a diameter of 1.75 mm, manufactured by SunLu, was used for this study. There is no specific PLA or TPU as the filaments are directly obtained from the manufacturer in a spool form.

b) Porosity analysis was conducted using a densimeter due to the lack of porosity equipment at the laboratory. The Archimedes Principle was explored in this method, where less density indicates a higher porosity level.

c) The humidity level was decided through four conditions as follows:

i. New PLA-TPU filament roll, which acts as the reference (control).
ii. PLA-TPU filament roll stored in the vacuum bag with 50g silica gels.
iii. PLA-TPU filament roll stored in the vacuum bag without silica gels.
iv. PLA-TPU filament roll stored in an open environment, exposed to a humidifier for a variant of 48, 96, and 150 hours. The printing parameters for all conditions were similar, with three replications of each conditional setting.

d) A house humidifier was employed for the humidity-exposure purpose, but the time (day/night) and ambiance temperature during the exposure for each condition was not controlled. Therefore, the study only considers the duration of exposure instead.

e) The composition of the sputter-coated material used was gold (Au) 80% and palladium (Pd) 20%.

f) Due to the FTIR chamber's size limitation, the dimension of samples was set to 10 mm to 10 mm (W x L) for both PLA-TPU filaments.

g) This study aims not to solve the humidity problems but to observe the polymer chain's structural changes when thermoplastic polymers are exposed to moisture. Therefore, it is hoped that the output of this study could create awareness among the FDM 3D printer users concerning the importance of storing their filament correctly.

1.5 Significance of Study

This work contributes to the analysis and examination of the influence of moisture on the chemical properties and to observe whether the chemical bonding changes or not when water is exposed to PLA and TPU filaments. If it is discovered that humidity influences the quality and characteristics of the printed components, a clear message emphasizing the need for proper storage of the used 3D printer filament can be sent. As a result, it may increase the print quality of PLA and TPU components and minimize PLA and TPU waste. Additionally, lowering 3D printing waste can help promote sustainable 3D printing since the number of 3D printer users continues to grow because of their affordability, flexibility, and ease of use.

This research demonstrates that if humidity interferes with chemical bonding and alters chemical properties and printing quality, in that case, we will educate FDM 3D printer users on how important it is to control used filaments from being exposed to humidity. Then, when silica gels are used in this study, suppose the use of desiccant in a vacuum bag is sufficient to control the humidity level, in that case, we can advise 3D printer users to use this method as an alternative to the drying rack, which is quite expensive for some FDM users. Thus, it is intended that this study would demonstrate the influence of humidity on the printing quality while also raising awareness among all 3D printer users.

1.6 Organization of the Report

Five chapters are included in this study: an introduction, a review of the literature, a methodological section, results and discussion, and a conclusion and suggestion. Chapter 1 began with an overview of the study's context, problem statement, objectives, and scope. Chapter 2 summarises prior research or reflections on the FDM technique, PLA and TPU filaments, the effect of humidity on 3D printed components, and the chemical properties testing method. Chapter 3 discusses the applied methods for attaining the specified objectives. Later in Chapter 4, the chemical characterization, Archimedes principles, and the findings of the SEM investigation are discussed. Finally, Chapter 5 detailed the study's conclusion and suggestions.

CHAPTER 2

LITERATURE REVIEW

This chapter explains the theory and fundamentals related to the study. The data gathered from articles, journals, published literature, books, magazines, etc., focus on the 3D printing technology of the FDM process. Furthermore, this chapter reviews PLA-TPU materials, including their production and properties. Humidity and its influence on 3D printing parts are also enclosed in this chapter. Besides, the FTIR analysis, porosity analysis using Archimedes concept, and SEM analysis are discussed.

2.1 Overview of 3D Printing

Charles Hull was the first person to commercialize 3D printing in 1980. However, when it comes to 3D Printing, the process of creating three-dimensional structures directly from computer-aided design (CAD) models has evolved. As a result, printing has become a unique and adaptable technology (Shahrubudin, Lee and Ramlan, 2019).

As the material is added to a geometrical representation, 3D Printing creates physical objects. Therefore, various materials can be used in 3D printing to create very complicated geometrical pieces for a wide range of applications. For example, 3D components for medical, construction, engineering, and educational purposes are built using metals, alloys, ceramics, polymers, composites, biomaterials, and concrete. As a result, songs on raw materials have become increasingly beneficial (Xu et al., 2021).

Materials extrusion and material jetting are all included in the ASTM Standard F2792. Other additive manufacturing methods covered in the standard are powder bed fusion and vat photopolymerization. Now that 3D printing has become more widespread, it can make a wide range of products, not just prototypes (Wei et al., 2020). Open-source designs and mass customization are becoming more commonplace in domains such as agricultural, healthcare, automotive, and aerospace industries thanks to 3D Printing (Lee et al., 2019). High-quality materials that fulfill consistent standards are essential for producing high-quality devices in 3D printing. Therefore, material control processes, requirements, and agreements between suppliers, buyers, and end-users are formed to assure this. As a result, 3D Printing can now create various materials such as ceramic, metal, and polymer and composites and functionally graded materials derived from these materials.

2.2 Fused Deposition Modelling (FDM)

Extrusion structures are made using FDM, a 3D printing method that utilizes filament as a starting point. Fused deposition modeling (FDM) is a widely accepted AM process for three-dimensional manufacturing components for layering material through a liquefier nozzle with an X-Y movement (Rajpurohit and Dave, 2018). FDM technologies are a subset of the community of extrusion-based 3D printers (Vyavahare et al., 2020). As a result, fused Deposition Modeling (FDM) is becoming increasingly popular for modeling, prototyping, and manufacturing applications. The fused deposition modeling (FDM) technique is visualized in Fig 2.1 (Klippstein et al., 2018).

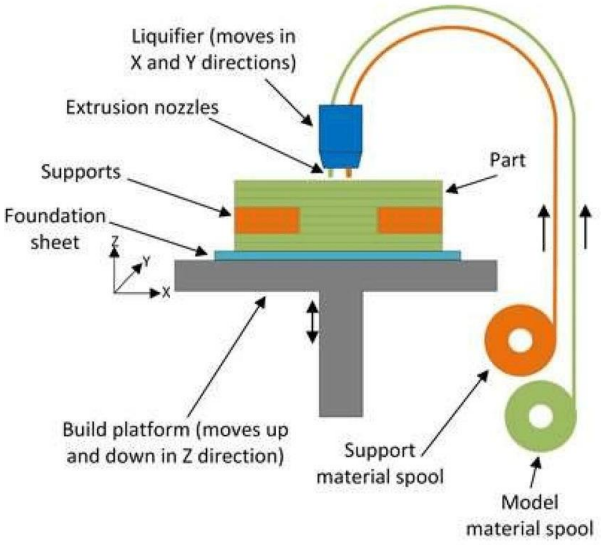

Figure 2.1: Schematic of FDM process (Klippstein et al., 2018)

FDM is primarily utilized to produce Acrylonitrile Butadiene Styrene (ABS), polyamide, polycarbonate, polyethylene, and polypropylene (Wasti and Adhikari, 2020). In addition, our materials like silicon nitrate, PZT (Plain Zinc Triazine), and Aluminum Oxide are still utilized in the FDM process (Zhang et al., 2020).

2.2.1 Process Parameters

Today, additive production processes like FDM are needed to provide superior component efficiency, high efficiency, protection, low production cost, and shorter time. Each design's additive production process conditions must be calculated to satisfy consumer requirements and satisfaction. The primary performance of the additive production process relies on the appropriate set of process parameters (Mohamed et al., 2021).

It is important to set optimal process conditions as it leads to higher consistency of product, increased efficiency, improvement in the dimensional accuracy, elimination of unacceptable waste, and significant scraps. It also reduces the time and costs of production. However, due to various contradictory parameters that affect the component's consistency and material properties, the optimal parameters must be carefully chosen to achieve the best results with FDM. Nevertheless, Masood (1996) stated that the correct

selection of process parameters could calculate the quality of the part and mechanical properties of the parts produced. FDM process parameters cause and effect fishbone diagram (see Figure 2.2).

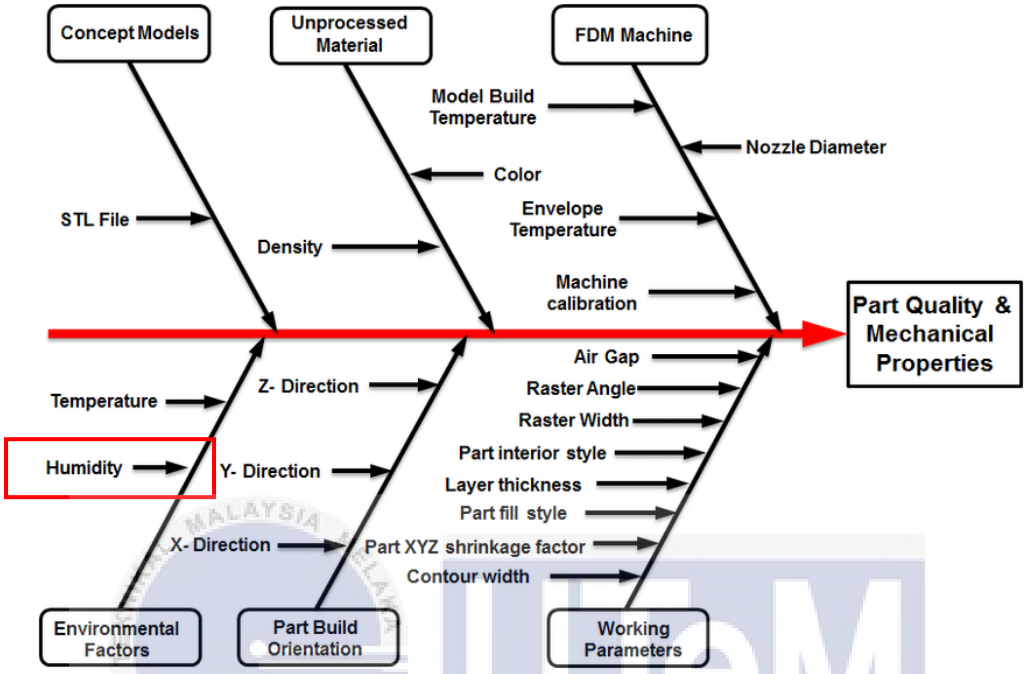

Figure 2.2: FDM Process Parameters Fishbone Diagram of Cause and Effect (Omar Ahmed Mohamed, 2019)

2.3 Polylactic acid (PLA)

Wallace Carothers, who was also responsible for the invention of nylon, discovered polylactic acid (PLA) in the 1920s. He worked with DuPont to create less harmful plastic for the environment. The commercial application of PLA, on the other hand, proved prohibitively expensive. In their research, PLA was made cheaper by Inkinen et al. (2011), using renewable ingredients like maize starch and sugarcane. As a result, it may be easily recycled and biodegradable under the right conditions. Composting plastic scraps at 140 degrees for ten days would be an example of a facility where bacteria turn plastic waste into fertilizer (Soares et al., 2018).

Additionally, PLA plastic is frequently used in 3D printing as a filament to create 3D printed things. First, the user creates a three-dimensional model in three-dimensional software, converted to a different format by the three-dimensional printer's interface software. This software segments the model and determines how the printer will print the layers. Then, after melting the PLA plastic filament, it is extruded via a heated nozzle, which places it in a single layer. As the plastic cools, it becomes more challenging. Finally, the following layer is printed, and the process is continued until the part is complete (Algarni, 2021).

PLA is a plastic substance frequently used to build models and prototypes of solid items and components. In addition, it is a thermoplastic polyester resin that is used as a raw material in additive manufacturing techniques and applications such as 3D printing. When it comes to 3-D Printing, PLA is next behind ABS as the most often used plastic raw material (Woern et al., 2018).

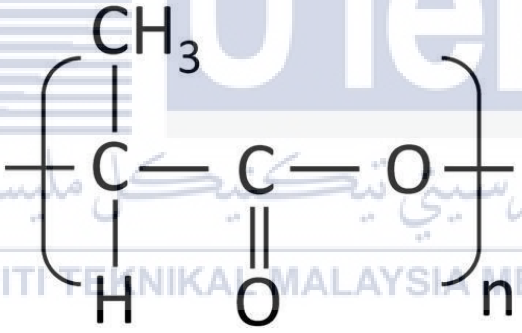

Figure 2.3: PLA chemical structure (Cubas-Cano et al., 2018)

Figure 2.3 shows the PLA chemical structure for references to the researcher Cubas-Cano et al. (2018) of PLA. Consequently, as illustrated in Figure 2.4, PLA is a biodegradable polymer created from renewable sources such as beets and maize.

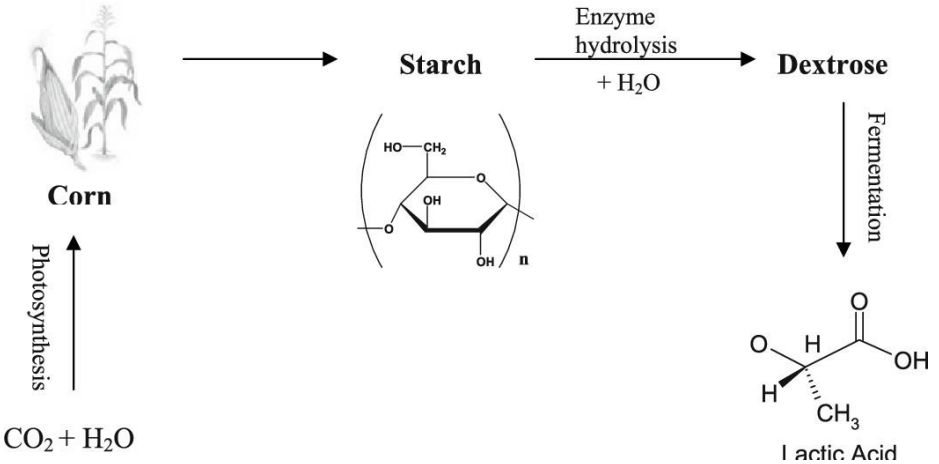

Figure 2.4: Lactic acid production from a renewable source ("Poly Lactic Acid & Collagen Fiber" n.d.)

2.3.1 Production of PLA

Lactides are commonly employed to convert PLA into a petrochemical component in its overall form. Agricultural items can also be fermented to produce significant quantities of this chemical (Bhandari et al., 2019).

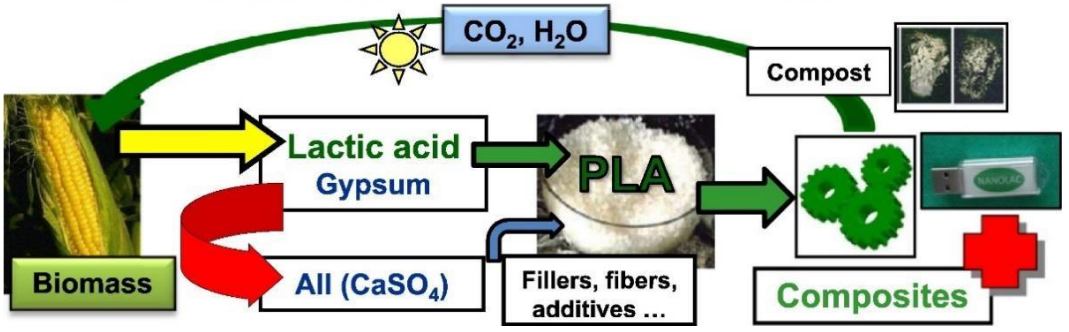

Figure 2.5: Production of PLA (Murariu and Dubois, 2016)

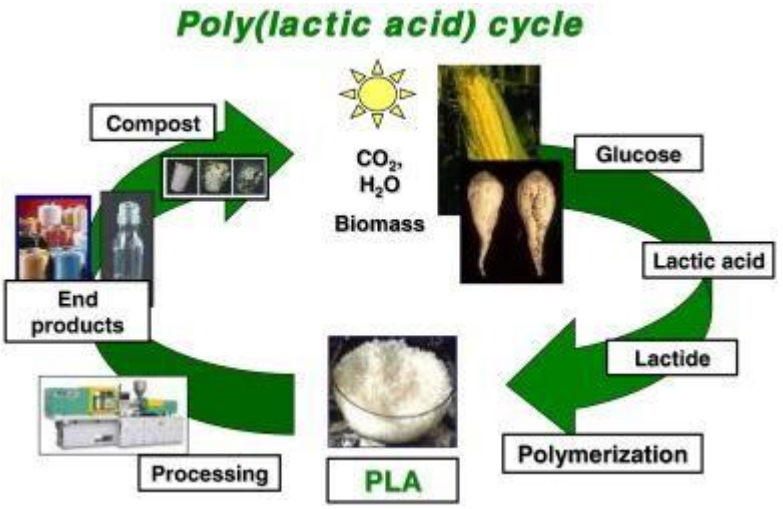

Figure 2.6: Poly (lactic acid) cycle (Murariu and Dubois 2016)

Figure 2.5 shows the flow production of PLA, and Figure 2.6 illustrates the PLA cycle. Based on researchers, it was expected that 3D printed PLA material might be recycled once (Sanyang et al., 2015).

According to Meng et al. (2015), PLA processing entails synthesizing and polymerizing lactic acid monomers. L-lactic acid and D-lactic acid are the two enantiomers of lactic acid (HOCH3CHCOOH). The L isomer rotates clockwise in the polarised light plane. By contrast, the D isomer rotates anticlockwise.

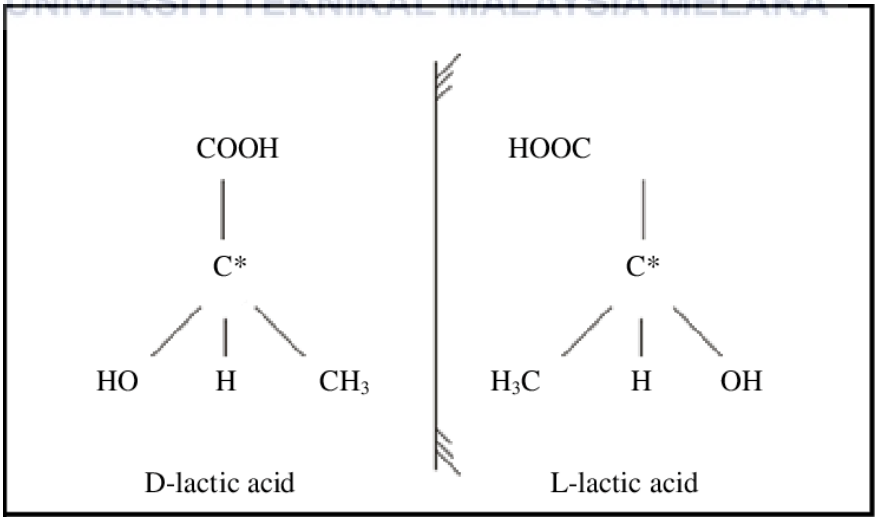

Figure 2.7: Optical isomers of lactic acid (Casalini et al., 2019)

The two methods for polymerizing lactic acid (lactide) into high molecular weight PLA are direct lactic acid polycondensation (LA) and ring-opening polymerization (ROP) employing the cyclic dimer (Lopez-Anido et al., 2019). Additionally, Figure 2.8 stated that condensation of azeotropic dehydration could create PLA.

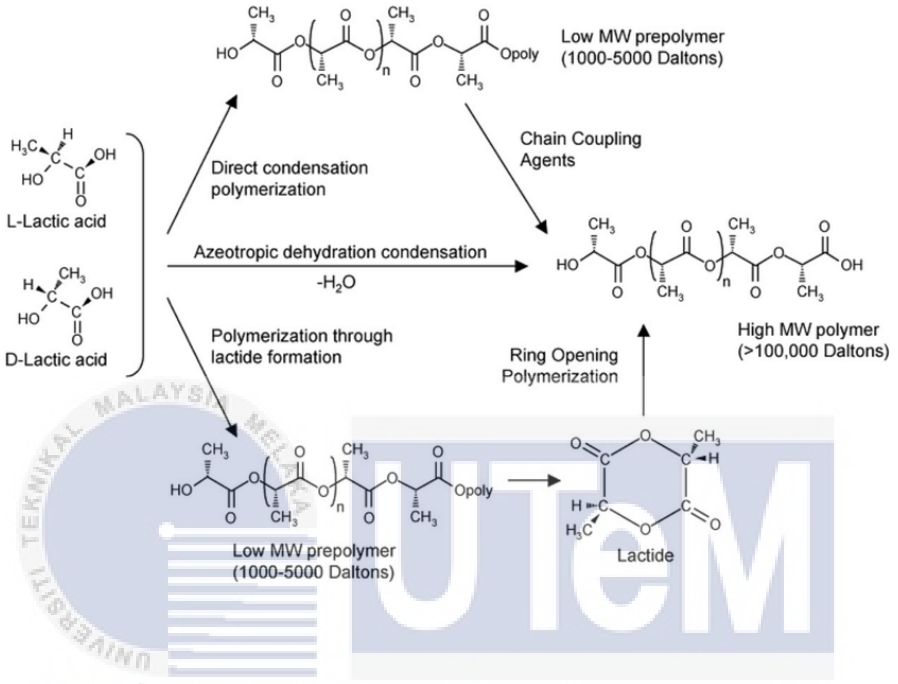

Figure 2.8: Polymerization steps of PLA (Ameen and Caruso 2017)

Gardner et al. (2019) state high vacuum and temperatures are necessary for direct lactic acid polymerization. A solvent will be used to remove the water generated by the condensation reaction. Carothers utilized this technique in the production of PLA polymers. Due to the difficulties associated with eliminating water and contaminants, the produced chemical seems to have a low or moderate molecular weight (Mw 10,000- 20,000). In mild conditions, lactide forms as a cyclic dimer as water is drained from a solution without using a solvent. Polymerization of ring-opening (ROP) through a cyclic dimer (lactide) using a stannous catalyst on an octoate base is typically used to produce PLA with a high molecular weight. Other motives and polymerization processes, on the other hand, are used in laboratory demonstrations.

Additionally, the production of PLA by enzymes is a novel endeavor for research and industry (Algarni, 2021). Azeotropic polycondensation and specific catalysts enable the

manufacture of PLA polymers with high molecular weights. Furthermore, the distillation pressures can be reduced by adding molecular sieves to the azeotropic solution, and PLA can be separated from the solvent. The stimuli's range and content, the proportion of solvent volume, and the reaction time for PLA production have all been investigated. The findings 15 demonstrated that it is possible to reach a molecular weight of 6.6 104 g/mol of PLA by utilizing improved laboratory instruments, the suitable complex catalyst, and the correct solvent volume ratio (Jamshidian et al., 2010).

2.3.2 Properties of PLA

PLA shares many of the features of many different synthetic fibers because it is a melt-processable vegetable fiber. For example, a white powder made of lactic acid homopolymer has a glass transition temperature (Tg) of 55°C and a melting temperature (Tm) of 175°C when it is at room temperature. In addition, because of its significant molecular weight, PLA is a colorless, glossy, solid thermoplastic composite with properties like polystyrene (Lv et al., 2018).

Table 2.1: Chemical properties of PLA (Xiao et al., 2012)

Properties	PDLA	PLLA	PDLLA
Crystalline structure	Crystalline	Semi-crystalline	Amorphous
Melting temperature (°C)	~ 180	~180	-
Glass transition temperature (°C)	50-60	55-60	Variable
Decomposition temperature (°C)	~200	~200	185-200
Elongation at break (%)	20-30	20-30	Variable
Breaking strength (g/d)	4.0-5.0	5.0-6.0	Variable
Half-life is 37°C normal saline	4-6 months	4-6 months	2-3 months

According to Table 2.1, PDLA, PLLA and PDLLA are soluble in various solvents, including benzene, chloroform, acetonitrile and dioxane. Ethanol, methanol, an aliphatic hydrocarbon, on the other hand, are insoluble in them. The half-life of PLA in the atmosphere varies from 6 months to two years, depending on particle size and shape, isomer ratio, and 16 temperatures. PLA's melting temperature (Tm) and glass transition point (Tg) decrease as the number of PLLA decreases. Tg determines the PLA's physical properties, including density, thermal, mechanical, and rheological qualities. PLA appears to be crystalline when the PLLA value exceeds 90%, whereas the less optically pure PLA is typically amorphous (Henton et al., 2005). Thus, Tg and Tm are critical physical characteristics that help predict how semicrystalline PLA will behave.

Enantiopure PLA has a melting enthalpy of 93 J/g at 100% crystallinity (H°m). The molar mass of the polymer, the ambient temperature, and the polymer's purity all affect the Tm and crystallinity values. There were two different densities listed for the amorphous and crystalline forms of PLLA. There are four types of PLA: crystalline, unstructured, and L-lactide. The crystalline PLA density is 1.36 g/cm3, the amorphous PLA density is 1.25 g/cm3, and the L-lactide density is 1.36 g/cm3 (Farah et al., 2016). After months of contact with moisture, PLA degrades predominantly by hydrolysis in two distinct ways.

To begin, the molecular weight of esters decreases due to the spontaneous non-enzymatic chain breakage. Then, as a second benefit, the oligomers' molecular weight is lowered before the lactic acid consumes them, and bacteria naturally break them down to produce carbon dioxide and water. Third, the polymer itself dictates the rate of disintegration. The speed of polymer breakdown is affected by particle size and shape, temperature, moisture, crystallinity, percent isomer, residual lactic acid concentration, molecular weight and water diffusion, and catalyst metal impurities (Lasprilla et al., 2012). Several of PLA's physical features are summarized in Table 2.2.

Table 2.2: Physical properties of PLA (Gupta et al. 2007)

Sr. No	Property	Values	Units
1.	Viscosity of PLA	0.265-0.467	M Ps-s
2.	Density of PLA	1.25	gm/cm³ at 21.5 °C
3.	Thermal conductivity	0.13	W/M0k
4.	Conduct diffusivity	0.056	m²/sec
5.	Specific heat	1800	J/Kg0K
6.	Feed rate	2.247-2.67	m/sec
7.	Yield Tensile Strength	52	(MPa)
8.	% Elongation at Yield	10-100	%
9.	Flexural Modulus	345-450	(MPa)
10.	Melting point	120-170	(°C)
11.	Glass transition temperature	54-56	(°C)
12.	Shear Modulus	2.4	GPa

PLA exhibits a high degree of hydrophilic. Most thermoplastic polymers, including nylon, polyethylene terephthalate (PET), and Polypropylene (PP), have lower hydrophilicity than PLA because water molecules can access the polar oxygen bonds in its molecules. As a result, it enhances the fiber's wettability and moisture vapor transport. According to Bellehumeur et al. (2004), while PLA fibers are not as humid as cotton, they may increase moisture transfer when used in place of polyethylene terephthalate (PET) or nylon fibers. Furthermore, PLA is more alkaline-resistant than polyethylene terephthalate (PET).

2.4 Thermoplastic Acid (TPU)

Formed by combining the mechanical qualities of rubber and thermoplastic polymers, TPUs are known as thermoplastic elastomers (TPEs). Because they lack the chemical networks seen in rubber, they may be melted and treated repeatedly without breaking down. TPU was the world's first processable homogeneous thermoplastic elastomer. Thermoplastic elastomers continue to play an essential role in today's ever- expanding family of

thermoplastic elastomers, with applications in practically every industrial sector (Frick and Rochman, 2004).

Thermoplastic polyurethane (TPU), a polyurethane substance resistant to oil, grease, and abrasion, has many properties, including thickness and transparency. They are thermoplastic elastomers made of linear segmented block copolymers with alternating hard and soft segments (Aurilia et al., 2011).

Dynamic mechanical spectra make it possible to distinguish between hard and soft segments in TPU based on their glass transition temperatures, which affects their miscibility (Tg). The loss modulus spectrum of an immiscible TPU typically exhibits two peaks, each corresponding to the glass transition temperature of a different component (Tg). If the two parts are miscible, TPU will have a single wide increase between the two original glass transition temperature (Tg) peaks (Liu et al., 2018).

Because of their tremendous attraction, they have gathered and organized themselves well throughout this stage. Within the soft and flexible matrix, crystallization or pseudo-crystalline zones appear. What's known as polarity and molecular weight adjustment may have a significant or minor effect on this so-called phase difference between the two blocks (Fallon et al., 2019). TPU's crystalline or pseudo-crystalline components contribute to the material's high elasticity and act as physical crosslinks. On the other hand, the flexible chains will transmit the polymer's elongation properties.

On the other hand, heat breaks these "pseudo crosslinks," As a result, these materials may be produced using typical extrusion, injection molding, and calendaring methods. TPU scrap can thus be reused and repurposed. When various kinds of nanofiller are applied, it has been shown that many production techniques such as in situ polymerization melting blend, solution mixing, and solvent exchange processing can improve TPU features (carbon nanofibrils, carbon nanotubes, organo-modified silicates, and nano- silica). Tear strength, abrasion resistance, thermal stability, mechanical characteristics, and barrier qualities have been improved in TPU-based nanocomposites (Cui et al., 2020).

2.4.1 Production of TPU

IG Farben's laboratory at Leverkusen, Germany, produced thermoplastic polyurethane (TPU) in 1937, led by Otto Bayer and his colleagues. These compounds are formed by a polyaddition reaction in one or more diols and diisocyanates (H. Chen et al., 2020). For a TPU, the following three essential ingredients are required:

a) Polyols, also known as long-chain diols, are a form of long-chain diol.
b) A chain extender is also referred to as a short-chain diol.
c) A diisocyanate is a segmented linear segmented block copolymer that is complex and soft.

With a polyol and isocyanate, the Soft Segment (polyether or polyester) has the flexibility and elongation of TPU. The hard segment (aromatic or aliphatic), which includes a chain extender and an isocyanate, accounts for TPU's toughness and physical performance.

a) Aromatic TPUs that are isocyanate-based, such as MDI
b) Isocyanate-based aliphatic TPUs such as H12 MDI, HDI, and IPDI

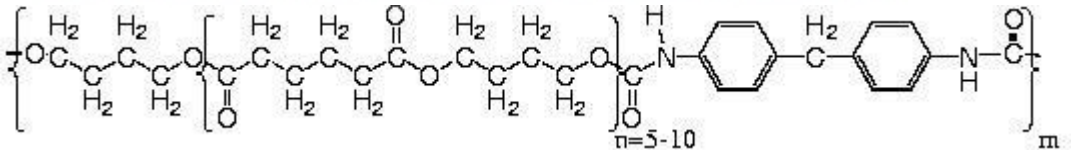

Figure 2.9: Molecular Structure of TPU (Marino et al., 2011)

2.4.2 Properties of TPU

Table 2.3: Properties of thermoplastic polyurethane (TPU) (Zahid et al., 2020)

Properties	Test Method	Units	Typical Value
Density	ASTM D792	lb / in3	0.0426
Hardness, Shore A	ASTM D2240	-	67
Tensile Strength	ASTM D412	psi	2900
Elongation at break	ASTM D412	%	700
100% modulus	ASTM D412	psi	435 @ Strain 100%
300% modulus	ASTM D412	psi	725 @ Strain 300%
Tear Strength	ASTM D624	pli	371
Abrasion	DIN Abrasion Loss; DIN 53516	-	40
Glass Transition Temp, Tg	DSC	ºC	-42.0

2.5 FDM 3D Printer Materials

There are many typical additives used in additive production: plastic, metal, sand, wax, and many more. According to Ahmad et al. (2020), 3D printing materials majority are used plastics and metal. Moreover, ceramics and composites are used, other than a wide variety of investigated and tested materials for 3D printing. Depending on applied additive manufacturing (AM) technology, plastics are frequently used for 3D printing. Usually, researchers are more focused on the adverse effects of pollution and waste. Thus, the concept of "eco-friendly" biodegradable, recyclable and compostable materials was developed. After all, regardless of their low prices, non-biodegradable materials dominate the rapid prototyping materials market. The materials are typically rated in three ways: consistency, mechanical efficiency, and process. Next, the following material physical properties of major pure polymers used in the FDM technology over the past years are shown in Figure 2.10: strength, flexibility, and durability.

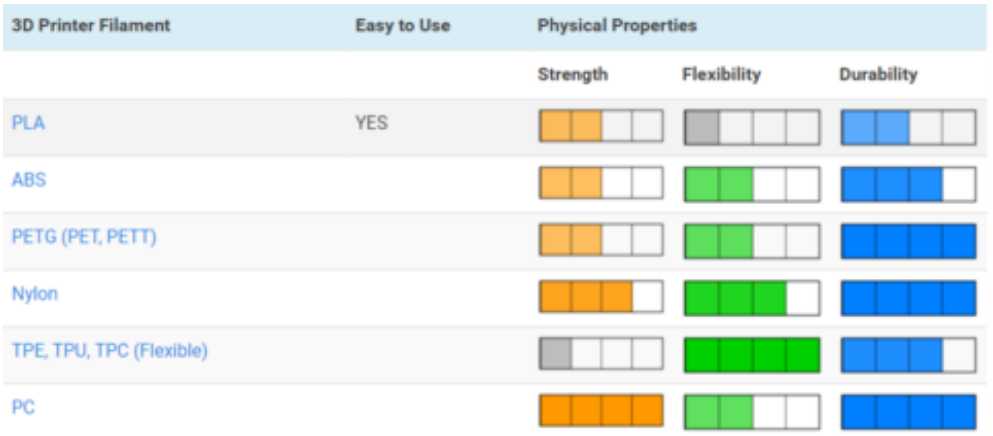

Figure 2.10: Comparison of thermoplastic materials (Müller et al., 2019)

Dey and Yodo, (2019) described the usually used filament materials as below:

a) PLA: A biodegradable thermoplastic, which is frequently used in FDM. Low energy and temperature requirements are necessary to generate high-quality prototypes and functioning parts. PLA filament is commonly used in desktop 3D printers because they don't need a heated bed, although a clogged printing nozzle might cause problems. PLA is tougher than ABS and has low tensile strength, warp, and flexibility. PLA-designed components required extra care compared with ABS for the post-processing.

b) ABS: Amongst the most popular materials applied to manufacture parts through FDM, a thermoplastic and amorphous polymer. It is a copolymer manufactured from acrylonitrile, butadiene, and styrene; ABS has two significant mechanical properties of impact resistance and hardness. In addition, ABS is not organically degradable but poses a decreased chance of jamming dust.

c) PETG & TPU: Materials like high-intensity polystyrene (HIPS, PPSF), polyethylene triphenyl glycol (PETG), or thermoplastics (TPU) are rarely used as filament materials, as are bio composites, ceramics, and other composites. These products are either still being produced or aren't readily available.

d) Nylon: The filament used to print parts with high flexibility and more durability. It is incredibly durable and resistant to impact, but it is heavily moisturized. Nylon is as much warp as ABS. Nylon retains atmospheric moisture when hygroscopic, just as many other filaments are seen in FDM. However, moisture accumulation deteriorates the features of the filaments and induces partial deterioration.

e) PC: A category of thermoplastics recognized for their resilience, strength, and hardness, with some being translucent. They are a commodity that is known for their high resistance. In addition, they are heat tolerant high-temperature thermoplastics, excellent layer for layer binding, and have a good surface consistency.

2.5.1 Silica Gels

Silica gel materials are the ones that can absorb moisture from the air, preventing condensation or moisture from damaging compressed air. Research conducted by Cao et al. (2019) shares their opinion that silica gel can hold 30 to 40% of water's mass since each silica sphere contains many tiny interconnecting pores due to its large surface area. Furthermore, silica gel is commonly used as a desiccant to extend the shelf life of filaments because of its high hydrophobicity (ability to repel moisture). In addition, Seng et al. (2020), found that silica of various sizes could be employed as a filler in other polymer matrices to enhance their mechanical properties.

Silica gel is a traditional desiccant that is available in porous, granular, and amorphous forms. It is produced by a chemical reaction between sulfuric acid and sodium silicate. Internally, Silica Gel is formed of a vast network of tiny pores that collect and hold water, alcohol, hydrocarbons, and other substances through the processes of physical adsorption and capillary condensation. Except for the blue gel containing cobalt chloride, the white silica gel can be considered a food-grade product, except for the blue gel. It is commonly used in various products, including auto/spare parts, electrical appliances, electronics, food packaging, furniture, footwear, pharmaceutical, and nutraceutical products.

2.6 Influence of Humidity on 3D printing

The quantity of moisture present in the air is referred to as humidity. Relative Humidity (RH) and absolute Humidity (AH) are used to express this (RH). To determine the amount of water vapor in the air, the unit of measurement used is grams per cubic meter, or g/m3. The current temperature substantially influences absolute humidity. The AH is usual at low temperatures, but the air carries significantly more moisture at higher temperatures. Absolute humidity may be calculated as the mass of water vapor per volume of wet air (in grams per cubic meter) or water vapor per mass of dry air (usually in grams per kilogram). Water vapor mass per unit of gas volume (mg/liter or g/m³) is provided (Elvin, 2015).

Sometimes, relative humidity represents absolute Humidity near-maximal moisture at the same temperature. The ratio of water vapor accessible in the gas to the most significant amount of water vapor that the gas can create could be the ratio of water vapor (percent). The quantity of water vapor that a specific air volume can store increases as the temperature rises, resulting in a shift in relative humidity temperature. At 100 percent relative humidity, the atmosphere is wholly saturated with water vapor. Therefore, when the gas temperature falls, the overall volume of water vapor is produced, bringing the relative humidity above 100% and condensation.

Humidity is the amount of water penetrating a body or vapor in the atmosphere. Water is more important than food for all living things to exist. On the other hand, humidity is frequently a source of issues for non-living components since it causes the oxidation and destruction of many materials. In the case of 3D printing, more precisely in the filaments, high humidity may create a slew of issues, all leading to the same result: a 3D printing failure (Kaszynka et al., 2019).

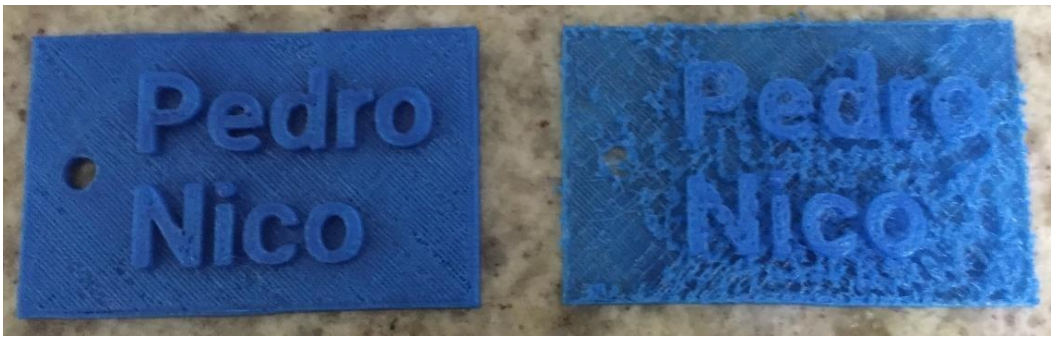

Figure 2.11: Humidity problem on 3D printing filaments (HUMIDITY ON FILAMENT - Google Search, n.d.)

Figure 2.11 shows the effect of humidity on 3D printed filaments. Attracting water can cause the following issues: increased fragility, larger diameter (potential problems with printers using a Bowden type extrusion system), filament degeneration, breaking filament, and so on. It is also crucial to realize that water-soaked filaments will have a greater extrusion temperature. Remember to keep the filaments out of the printer if there are not printing. They can become trapped in the extruder because they get fat and are more significant in diameter (Jantasee et al., 2017). Moisture in a filament can cause several problems, including:

a) Degradation of the filament: Intermolecular solid connections between the polymer and water molecules make the filaments hygroscopic, allowing them to absorb a lot of water. Internal micro-breaks can occur due to these linkages, weakening the filament structure.

b) Extruder / HotEnd jam: When the filament is heated in the HotEnd, the water in the filament evaporates, causing the filament to become a paste that clogs the barrel (Heat Break) or the nozzle. Using nylon filaments with high humidity (more than 20 percent) is a common cause of this issue.

c) Low-quality 3D prints (resistance and finishing): In 3D Printing, the combination of the parts leads to numerous mechanical and aesthetic issues. Water evaporation-caused gaps between layers are vulnerable stress locations where cracks can quickly form even with low force levels; when the high humidity level, the holes stated above produce a whitish surface.

2.7 Chemical Characterization using Fourier Transform Infrared Spectroscopy (FTIR)

The Michelson interferometer was crucial in developing the Fourier transform infrared (FTIR) technology we use today. Albert Abraham Michelson invented this essential piece of optical equipment**.** For Fourier transform infrared spectroscopy, the abbreviation FTIR is used, which is the preferred infrared spectroscopy method. Infrared spectroscopy is a technique in which infrared radiation is transmitted through a sample. The model absorbs around half of the infrared radiation while the rest passes through it (transmitted). Because the resulting spectrum depicts the molecule absorption and transmission of the sample, it can create a molecular fingerprint of the material. No two identical molecule configurations produce the same infrared range, just as there are no identical fingerprints. The researchers at Bacsik et al. (2004) stated that infrared spectroscopy could be employed for a wide range of diverse types of study.

FTIR can identify unknown materials and determine the quality or uniformity. It can also select the number of components included in a mixture. Fourier Transform Infrared Spectroscopy (FT-IR) investigations indicated that the soft domain interface substantially impacts the thermal and dynamic mechanical properties of TPU samples (Veerasingam et al., 2021). Figure 2.12 shows the diagram of the dispersive instrument and FTIR instrument. Next, Figure 2.13 shows the broadband source interferogram of FTIR.

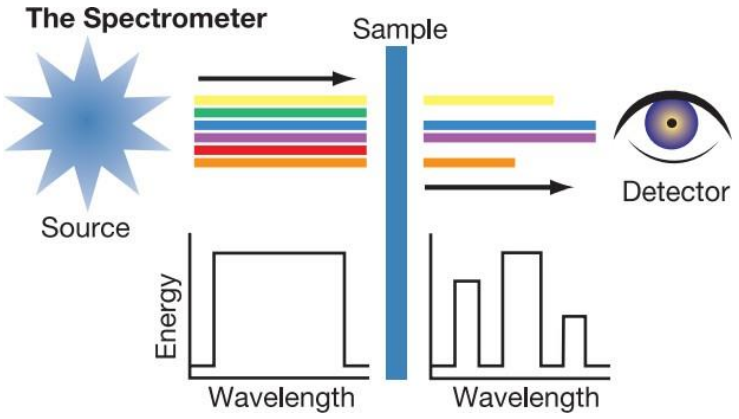

Figure 2.12: The dispersive spectral instrument and the FT-IR instrument are depicted in the diagram (Theakstone et al., 2021)

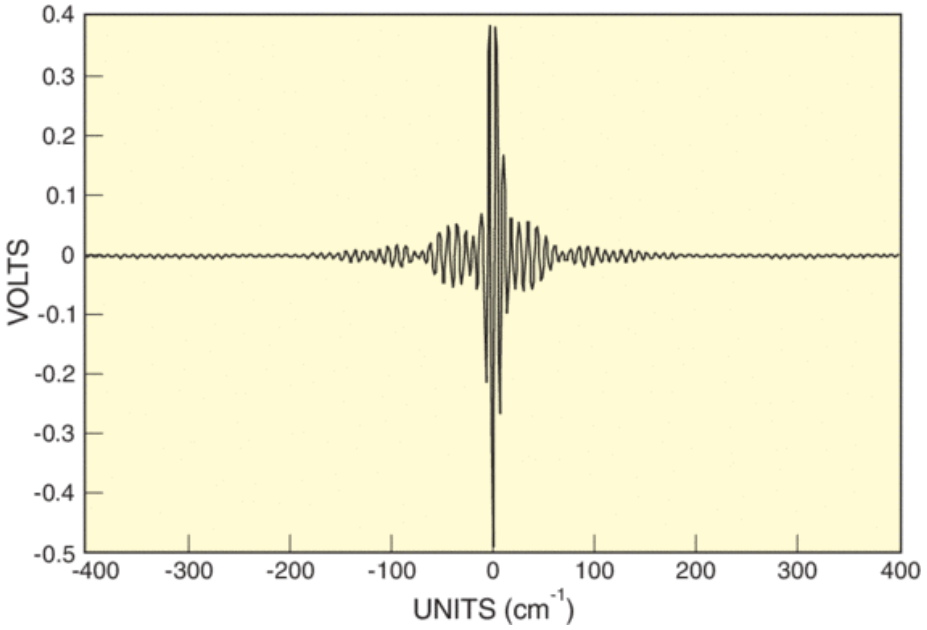

Figure 2.13: Broadband source interferogram (Kowalski et al., 2018)

It is necessary to convert an interferogram into a spectrum after it has been collected (emission, absorption, transmission, etc.). The shows Fast Fourier Transform algorithm is used to perform the conversion. In 1965, J.W. Cooley and JW Tukey discovered this technology, and since then, computing power has exploded at an accessible price, propelling FT-IR equipment into the mainstream market.

A series of processes calculate the spectrum. Phase correction and apodization must be performed to deal with instrument defects and scan restrictions. Some spectrum components have different time or phase delays, leading to inaccurate results. It is used to adjust the generation of fake spectral features created when the scanning process is truncated at its limitations (Indrayanto and Rohman, 2020).

To get high resolution using FT-IR, one must divide the possible optical path difference by the resolution limit. So, an OPD-capable FTIR scanner like our model 80351 can obtain a resolution of 0.5 cm-1. Table 2.4 shows that dispersive spectroscopy's resolution is frequently expressed in terms of wavenumbers and nanometers.

Table 2.4: Nanometer and Wavenumber Scales for Resolving Power (Rosi et al. 2019) 2019)

Wavelength (µm)	Resolution (Cm^{-1})	Resolution (nm)
0.2	1	0.004
0.5	1	0.025
1	1	0.1
2	1	0.4
5	1	1.0
10	1	10
20	1	40

2.8 Archimedes Concepts (Porosity)

The density of the produced pieces was measured using Archimedes' technique, which the Greek philosopher developed. Therefore, the filaments' humidity during moisture exposure in various environments can be determined by densimeter measurements using Archimedes' formula (Slotwinski & Garboczi, 2014). There are numerous reasons why 3D Printed parts have pores, and they all harm the part's overall performance. Therefore, the sintered samples' t density and porosity were assessed using an Archimedes-based densimeter (MH-300A, Matsuhaku, Taiwan) based on the Archimedes method (Cui et al., 2020).

Samples' relative densities, porosities, and apparent porosities were calculated using theoretical density in deionized water using the Archimedes technique. A closed porosity can also be obtained by removing apparent porosity from overall porosity (Y. Li et al., 2019).

According to Liao et al. (2019), the porosity and crystallinity of the printed parts are two characteristics that can influence the structural change of the printed parts. As a result, because the annealing was performed at 120°C and the melting point of the filament is approximately 150°C, there was no sign of porosity change.

2.9 Sputter Coating

Sputter-coating is an application technique that uses high-intensity lasers to deposit a skinny layer of material on a surface. It is possible to investigate the nanostructure properties of materials using a scanning electron microscope (SEM), which can be employed in many different applications. Some samples may be more difficult to scan than others, depending on their size and complexity. To put it differently, the procedure must be subjected to the sputter-coating process to obtain a high-resolution image. A variety of materials, both conductive and non-conductive, can be used to create sputter-coated surfaces. Sputter coating is typically performed in a vacuum chamber filled with either a chemically inert gas or a reactive gas, with the substrate positioned to face the target of the coating material. During the SEM method, a platinum (Pt) coating with an 8-nm thick layer is applied to the surface component to maintain a clear scanning image throughout (Jo et al., 2018).

2.10 Scanning Electron Microscope (SEM)

Material structure and plastic deformation processes may be studied and evaluated using scanning electron microscopy (SEM), a robust research technology for examining materials (Gussev and Leonard, 2019). Scanning Electron Microscope (SEM) is a technology that uses an electron focus beam to produce high-resolution images of a sample's microstructure. According to Kong et al. (2019), SEM microstructure scanning is the most used method. Surface composition, typography and morphology can be seen in an SEM image. Furthermore, through the scanning of a fracture component, this technology may be utilized to analyze the mechanical characteristics of 3D printed objects. According to a recent study by Hamid et al. (2019), surface images were acquired using a Carl Zeiss Evo 50 at 10.00kV accelerating voltage for 25x and 50x magnification power at secondary electrons.

The disintegration of the sample may be seen in the significant gaps in the SEM image, as discovered by Kakanuru and Pochiraju (2020). Using a Scanning Electron Microscope (SEM) Machine, the void geometry or microstructure of 3D printed PLA is shown in Figure 2.14.

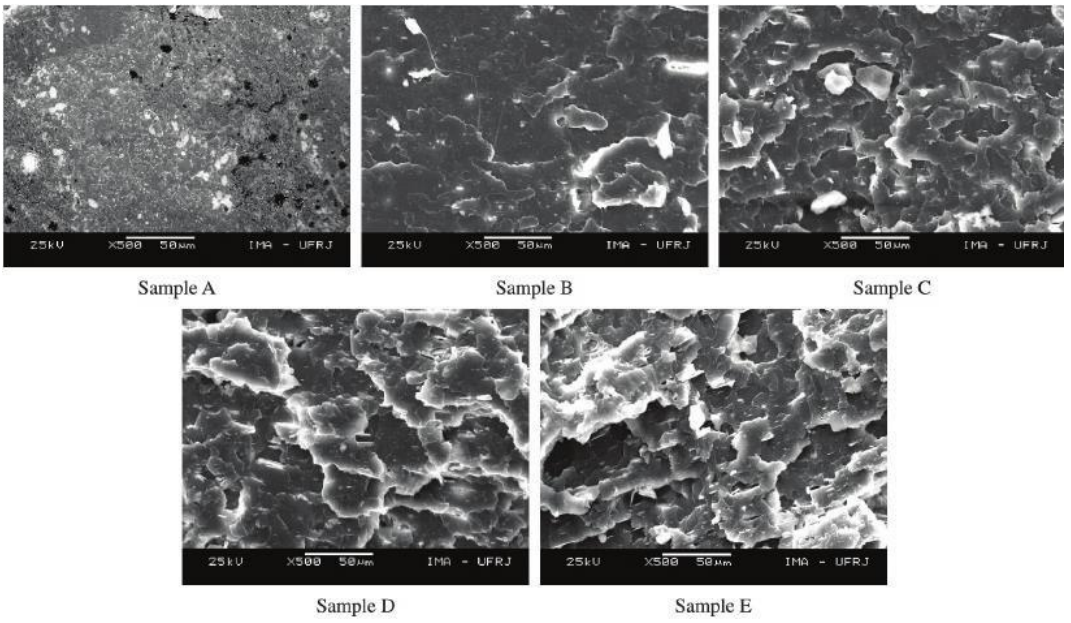

Figure 2.14: The microstructure of 3D printed PLA using Scanning Electron Microscope (SEM) Machine (Kakanuru and Pochiraju, 2020)

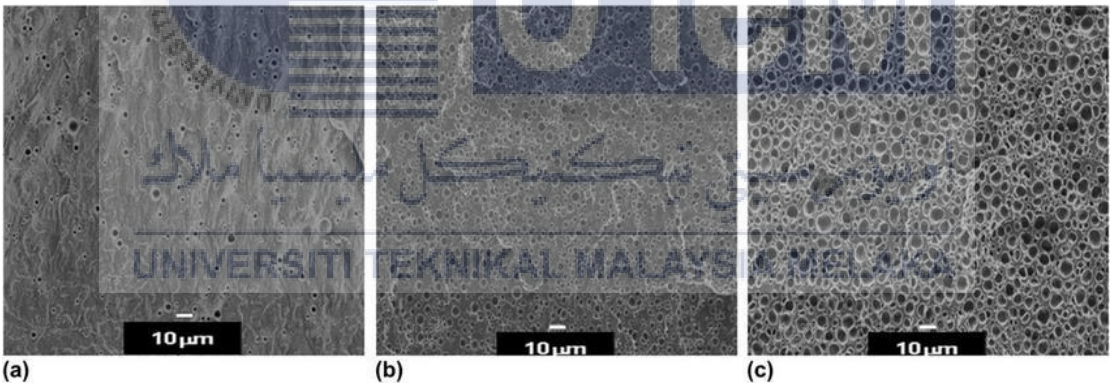

Figure 2.15: The microstructure of 3D printed TPU using Scanning Electron Microscope (SEM) Machine (Kakanuru and Pochiraju, 2020)

Zaldivar et al. 2018, examined initial filament moisture content to see how it affected the microstructure and mechanical performance of 3D printed objects in their research. Figure 2.15 illustrates the microstructure of 3D printed TPU using Scanning Electron Microscope (SEM) Machine.

2.11 Summary of Literature

In this chapter, there is still a gap in analysing the effect of humidity on the polymeric chemical chain, porosity, and microstructure of PLA and TPU specimens. However, some details are followed as a guide from the literature. To begin with, the PLA and TPU filaments were initially configured to be exposed to humidity for 150 hours, or roughly 6 days, using a humidifier. Secondly, the Ender 3 V2 3D printer was set to a speed of 60 mm/sec, a printing temperature of 220ºC, and a bed temperature of 60ºC for PLA and TPU specimens. Next, by using FTIR machines (JASCO FT/IR 6100) to detect the polymeric chemical chain for both PLA and TPU specimens. Besides that, the surface morphology samples were sputter-coated before SEM analysis. Lastly, this study examined the findings and compared them to the probability of the porosity effect of moisture exposed between PLA and TPU.

CHAPTER 3

METHODOLOGY

This chapter discusses the research methods and overall progress, including the essential methodologies for the investigation. The selected mode of analysis used, data collection, and optimizing the product were presented after referring to the technical specification and findings from the literature. The research plan is designed to achieve the stated objectives in Chapter 1, which are to identify the influence of water (H_20) in the polymeric chemical chain bonding using FTIR, to measure the porosity, and finally to observe the microstructural changes of the moisture-exposed 3D printed PLA-TPU filaments using SEM.

3.1 Overview of Methodology

The methodology process planning ensures that the study is planned accordingly. The procedures are developed based on the identified objectives, aiming to achieve the pre-set objectives in Chapter 1. Furthermore, this study combines both qualitative and quantitative methodologies. The secondary method collects qualitative techniques for the research by studying relevant books, journals, and articles. On the other hand, the quantitative process is the primary method, involving experimental and observational approaches.

3.2 Process Flow of the Study

The study consists of two parts, PSM 1 and PSM 2. It relies on three sections for PSM 1: an introduction, analysis of literature, and methods used to accomplish goals. PSM 2 focuses on implementing the research plan in PSM 1, which contains the 3D printing procedure, result and discussion, and conclusion, including the recommendation for any improvements. As depicted in Figure 3.1, the study's general flow continues from selecting the research title through its closing.

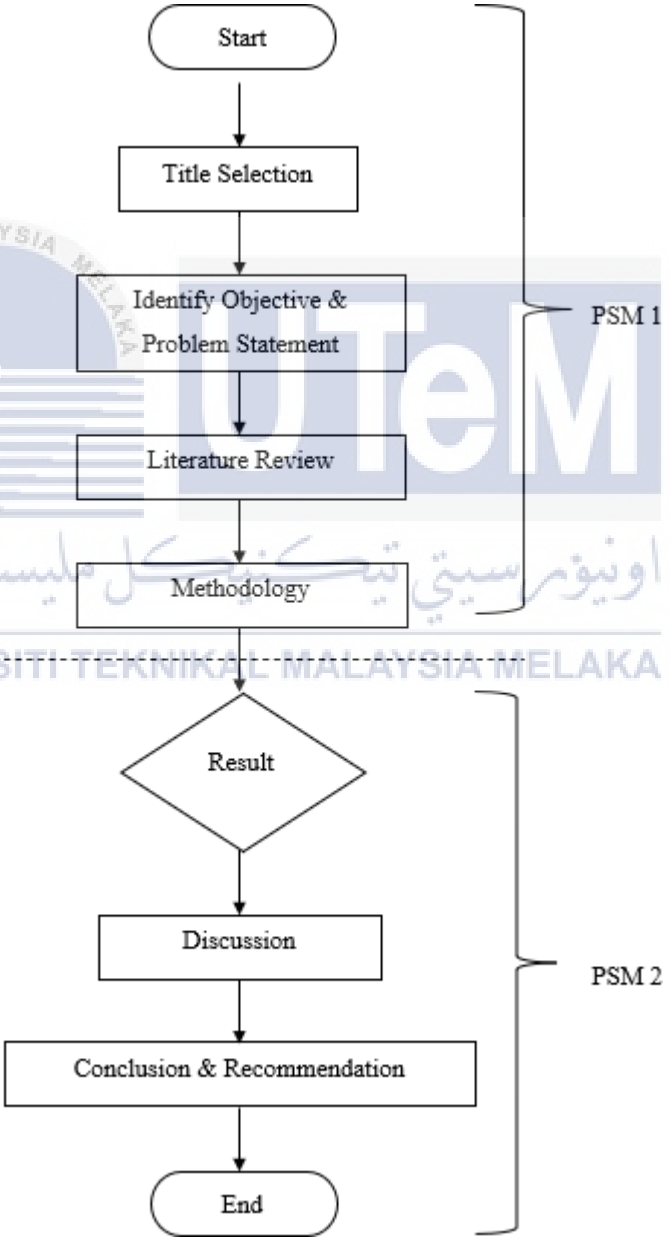

Figure 3.1: General process flow of PSM 1 and PSM 2

3.3 Relationship between the Objectives and Methodology

Table 3.1 shows how the study's objectives were accomplished by the approach used. As a result, this study was completed using the appropriate methods for each of the study's objectives, as briefly explained in this section.

Table 3.1: Implications of the methodology used in the study

Objective	Method
a. To identify the influence of water absorption (H_2O) in the polymeric chemical chain bonding of the humidity-exposed 3D printed PLA-TPU filaments using Fourier Transform Infrared Spectroscopy (FTIR).	FDM Process: • Machine (3D Printing): Ender 3 V2 3D Printer. • Material: PLA and TPU filaments • Filament Color: Red (PLA- TPU) FTIR Machine: • Fourier Transform Infrared Spectroscopy
b. To measure the porosity of the humidity-exposed 3D printed PLA-TPU filaments restructured under different humidity conditions using a densimeter (Archimedes Principle).	Porosity test: • Using densimeter (Archimedes concept)
c. To observe the structural changes of the humidity-exposed 3D printed PLA-TPU filaments through microstructure analysis using a Scanning Electron Microscope (SEM) machine.	Sputter-coating: • SC7620 Mini Sputter Coater machine SEM analysis: • Scanning electron microscope (SEM) machine

3.4 Flowchart of the Study

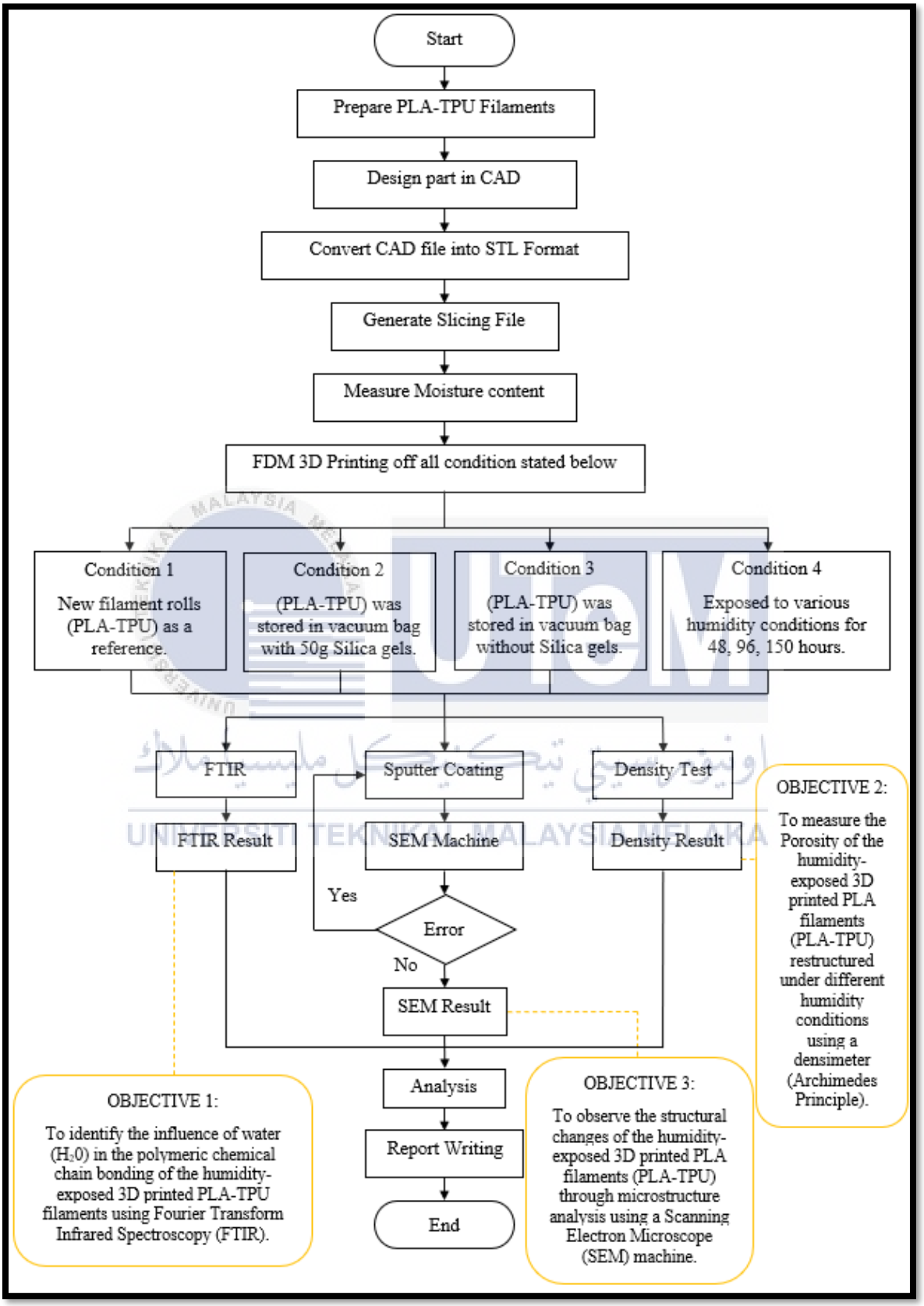

Figure 3.2: The research work flowchart

3.5 Preparation of PLA-TPU Filaments

Table 3.2: The materials used in this study are PLA and TPU filaments

Type of filament / Criteria	**PLA**	**TPU**
Filament Color	Red	
Filament diameter	1.75 mm	1.75 mm
Length	325 m	325 m
Weight	1 kg	1 kg
Manufacturer	SunLu	
Picture		

Figure 3.3: PLA filament

Figure 3.4: TPU filament

3.5.1 Conditions of each PLA-TPU filaments

The filament specification is shown in Table 3.2. The exposed condition decides the humidity level. Therefore, the filament will be exposed in four conditions; a) The new rolls of filament will act as the reference. b) The filaments will be stored in the vacuum bag with 50 g desiccant to maintain silica gel the dryness of the filaments. c) The filaments will be stored in the vacuum bag without silica gels 50 g desiccant silica gel. d) The filament will be stored in an open atmosphere and subjected to a humidifier for a period of 48, 96, and 150 hours. A humidifier is recognized as equipment used to enhance the humidity (moisture) level in one room or a whole building. Humidifiers are usually used to increase moisture content in the air, usually during the winter which the

air is dry. Thus, the purpose of using a humidifier in this study was to expose the PLA- TPU filaments to moisture before 3D printing to investigate if the existence of water influences the mechanical and microstructure of the 3D printed items.

3.6 CAD Model

CAD (computer-aided design) is an essential component of 3D printing. A 3D printer will not generate the necessary instructions to manufacture a sample or device without a CAD registration. Furthermore, the CAD model describes the amount of material that must be deposited by the 3D printer and where it must be deposited. As a result, a CAD model is used to accomplish 3D printing in this work. Besides, 3D specimens with dimensions in 10 mm illustrated in Figure 3.5 are used for the several conditions of humidity tests. The CAD model for 3D samples in Figure 3.6 is drawn using AutoCAD 2022 software.

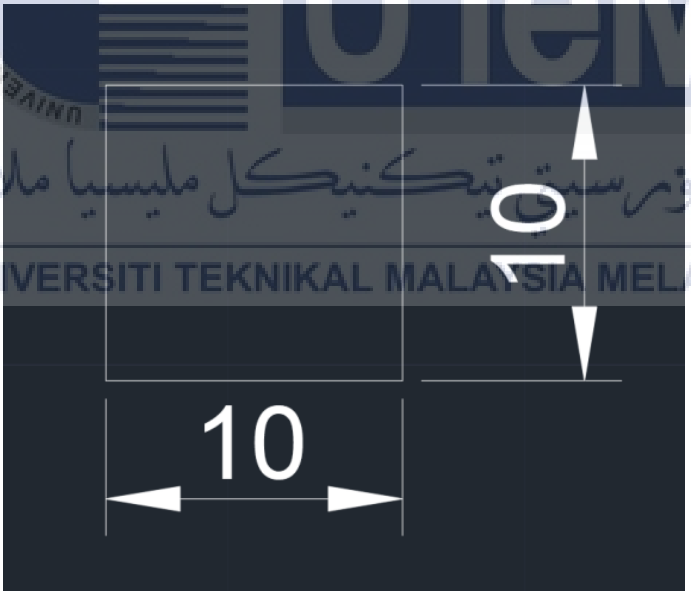

Figure 3.5: Specimens with dimensions in 10 mm x 10 mm

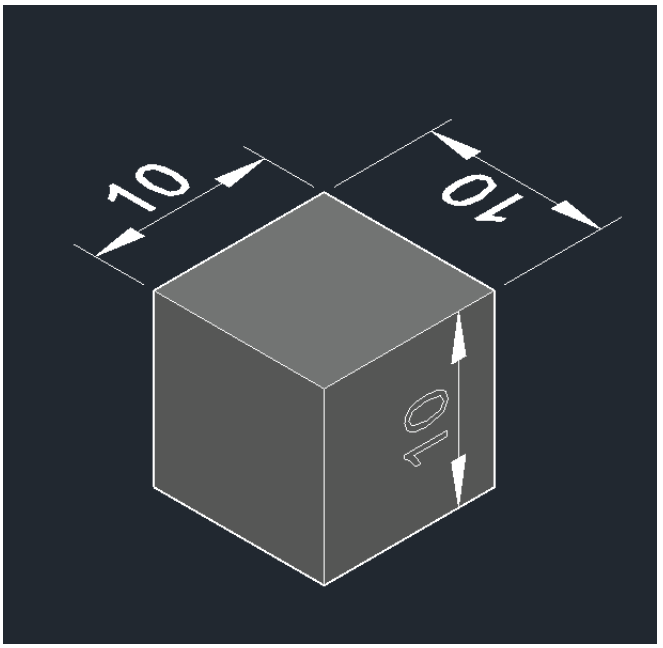

Figure 3.6: 3D specimens with dimensions in 10 mm x 10 mm drawn using AutoCAD 2022 software

CAD is converted into STL files (stereolithography format) to proceed with the 3D printing process. A pre-printer is a device that feeds an STL file into 3D slicer software, such as Flash Print. The platforms are in charge of generating G-code, which is the native language of 3D printers. It also enables the opening and positioning of several models on a printing bed. Thus, several models can be printed simultaneously, allowing printing management easier for the workplace.

3.7 FDM 3D Printing

The 3D Printing settings were kept constants for all samples, with a nozzle size of 0.4 mm and 70 mm per second printing speed. This study focuses on the FDM printing components using the Ender 3 V2 3D Printer, as shown in Figure 3.7. In addition, due to the machine's heated bed, the most common FDM defect, warping, may be prevented during the production process. Ender 3 V2 3D Printer comes with a hearable platform that can reach temperatures of 100°C. The build volume of the Ender 3 V2 3D Printer is 150mm × 150mm × 150mm. Thus, the machine has a slight build capacity making it ideal for printing specimens.

Figure 3.7: Ender 3 V2 3D Printer

3.7.1 Parameter Setting for 3D printing

Most FDM systems allow for adjusting several process variables, including nozzle and build temperature, printing speed, and layer thickness. Few setting parameters have been set to follow during the printing process. The process parameters will remain the same for all three conditions of PLA filaments used. According to Valerga et al. 2018, a better mechanical strength is achieved at a higher printing temperature of 220 °C. The printing temperature is first adjusted to 210°C, aligning with the 180-230 °C range recommended by Hsueh et al. (2021) for PLA printing. However, TPU can reach 220-250°C (Wang, 2020). Also, every printer is different regarding print speed, and ideal settings can depend on the type of printer used. However, PLA and TPU Printing are typically fine at any speed from 40mm/s to 70mm/s, with the recommended speed of 60mm/s (Nazir & Jeng, 2020).

Printing can achieve a better-quality output at a slower speed, which is more efficient. Print time and surface finish show the effect of layer thicknesses more clearly than the other. More excellent surface polish is achieved with thinner layers, but the print time increases. Thicker layers result in a worse finish but a faster printing time. FDM can create the most delicate layers that can be done with standard equipment that are usually 0.05 thick.

In addition, bed temperature is significant to allow materials to cool slower when extruded to prevent warping. It also gives added adhesion, meaning that the first layer holds well during printing, and the component is not released from the bed. Tyson (2018) stated 60°C as the best bed temperature for PLA. Wang (2020) noted 30 to 60°C as the best bed temperature for TPU. Other than that, it is recommended to use 100% as the filling percentage for a great result of mechanical resistance and quick printing (Álvarez et al., 2021). The process parameters for ODESSEY X2 SERIES for 3D Printing the PLA-TPU specimens are set according to Table 3.3

Table 3.3: The setting of process parameters for 3D printing

Material	Parameter setting
PLA	Printing temperature: 220 °C Bed temperature: 60 °C Printing speed: 60 mm/s Filling percentage: 100% Layer thickness: 0.10 mm
TPU	

3.7.2 Number of Specimen

Approximately 24 square-shaped samples were printed for both PLA and TPU filaments with four different conditions. The description of the type of PLA and TPU filaments and the number of specimens for the printing process is represented in Table 3.4. Three samples were divided into three analyses with three different conditions: FTIR analysis, density test, and SEM machine analysis, respectively.

Table 3.4: PLA-TPU filaments with the number of specimens printed for the study

Conditions of PLA-TPU Filaments		Number of Specimens	
		PLA	**TPU**
The new rolls of filament will act as the reference.		3	3
The filaments will be stored in the vacuum bag with 50 g desiccant to maintain silica gel the dryness of the filaments.		3	3
The filaments will be stored in the vacuum bag without silica gels 50 g desiccant silica gel.		3	3
The filament will be stored in an open environment and exposed to a humidifier for a variant of 48, 96 and 150 hours.	48	3	3
	96	3	3
	150	3	3

3.8 Fourier Transform Infrared Spectroscopy Analysis

FTIR analysis, also known as Fourier Transform Infrared Spectroscopy, is a method for detecting polymeric material. The FTIR method examines the chemical characteristics of test materials using infrared light.

Figure 3.8: FTIR Machine (JASCO FT/IR 6100)

The FTIR instrument emits infrared radiation that travels through the sample, where part of the radiation is absorbed and is transmitted. The sample molecules generate molecular rotation and vibrational energy due to their absorb radiation. As a result, the sample's molecular fingerprint spectrum may be seen at the detector's output. Spectral fingerprints uniquely identify chemicals, whether molecules or chemical structures.

FTIR spectroscopy was performed on all PLA-TPU filament samples. To ensure the equipment was thoroughly cleaned, isopropanol was used to clean the equipment. When handling the sample, both the crystal and the forceps were cleaned. Handling samples with the equipment to identify extremely minute contaminants necessitated gloves. Therefore, background data was gathered before collecting sample spectra since the findings might be impacted by human breath and air. Samples taken from the filaments will be trimmed to 10 mm x 10 mm for FTIR analysis.

3.9 Analysis of porosity using Archimedes' Principle

The Archimedes principle is applied to determine the porosity of the 3D printed filaments. The density of material was measured using the Archimedes approach for assessing the porosity of a substance. Despite the simplicity with which commercial gear can perform this activity, samples that allow for water penetration indicate that the sample is porous. Therefore, using the Archimedes method, a density measure is provided.

$$\rho = \left(\frac{M_a}{M_a - M_w} \right) \rho_W$$

Equation 3.1

Where,

M_a = mass of the sample measure in air

M_w = mass of the sample measure in water

ρ_w = density of water ($0.1 g/cm^3$)

In this study, the analytical balance scale measuring method with distilled water is employed to limit the occurrence of air bubbles. Using this equipment, it is possible to obtain precise mass measurements of samples in water and air. Each sample will be tested three times in the atmosphere and water based on stated conditions. Measuring is done once the scale has been re-calibrated. Each measurement result will be recorded once the scale has reached equilibrium. As seen in the Figure 3.9, this experiment requires an analytical balance scale sample tested three times in air and water. Measurements are taken once the scale has been re-calibrated. After the scale reaches equilibrium, each measurement result will be recorded.

Figure 3.9: Densimeter (Analytical balancing scale)

3.10 The Sputter Coating Process

Figure 3.10: SC 7620 Mini Sputter Coater

Figure 3.10 shows the mini sputter coater utilised in this study for sample analysis so that the SEM images could be of the desired quality. Sputter coating is a physical vapour deposition method that coats a sample with extremely thin, functional conductive metal layers, such as chromium, platinum, gold, or silver. The sputtering coat was used for sample analysis to obtain high-quality SEM images in this investigation. Because PLA and TPU materials are non-conductive, their surfaces serve as electron traps. Therefore, extra-white regions on the sample were caused by the concentration of electrons known as the charge on the surface. Because the conductive coating material acts as a conduit for the charged electrons to be expelled, high-quality SEM images can be obtained. The surface of the 3D printed components, PLA and TPU, were sputter-coated with 10nm of 20% palladium and 80% gold to enhance the SEM picture. Figure 3.11 shows the difference in SEM images for (a) before coating and (b) after coating.

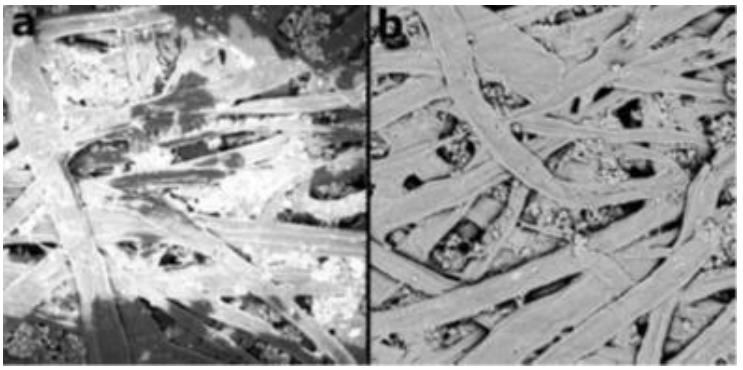

Figure 3.11: SEM images for (a) before coating and (b) after coating (Kakanuru and Pochiraju 2020)

3.11 Scanning Electron Machine Analysis

A material's strength is directly related to its microstructure. Therefore, the microstructural study is essential to determine how and why structural change occurs because the PLA-TPU filaments are exposed to moisture. In addition, the interface between filaments is studied after the sputter coating is completed. The material's microstructure is examined at magnifications of 50x and 100x using a Carl Zeiss Evo 50 scanning electron microscope (SEM) equipped with a 15 kV acceleration voltage as shown in Figure 3.12. A two-dimensional (2D) image is produced using a scanning electron microscope by directing an electron beam at a target and scanning it across the object. As electrons in the beam contact the sample, various signals are created, giving information about the sample's surface morphology and composition.

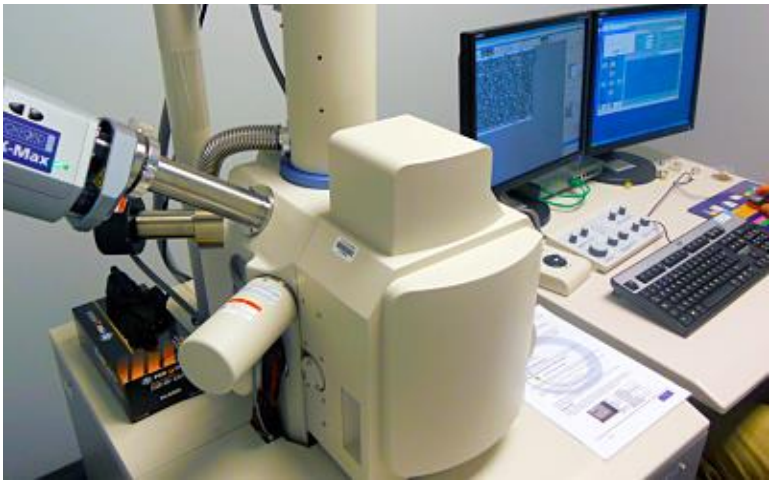

Figure 3.12: SEM machine (Carl Zeiss Evo 50)

CHAPTER 4

RESULT AND DISCUSSION

This chapter presents the analysis of polymeric chemical chain using FTIR; porosity analysis using densimeter; and structural analysis using SEM for all experimental conditions. Four conditions were set as follows: a) a new PLA-TPU filament (reference); b) used PLA-TPU filament stored in a vacuum bag with 50g silica gel; c) used PLA-TPU filament stored in a vacuum bag without silica gel; d) used PLA-TPU filament stored in an open environment and exposed to a humidifier for a variant of 48, 96, and 150 hours. The graph of transmittance vs wavenumber, the density test results, and the length of the surface morphology gap for all pre-stated conditions are evaluated, compared, and discussed.

4.1 3D Printing Process

In this study, the humidity and temperature of the environment were measured during printing to ensure there is no major difference while printing all the four conditions' specimens. The humidity level of the surrounding area was taken using a humidity meter before the printing process began, and the humidity was measured each time before printing each of the specimens. After averaging, the humidity level in the room is 88%, and the temperature is 27ºC.

Figures 4.1 and 4.2 show a sample of PLA and TPU filament 3D printed part with dimensions of 10m x 10mm x 10mm (WxLxH) printed with Ender 3 V2 3D printing. The figures show their isometric and top views.

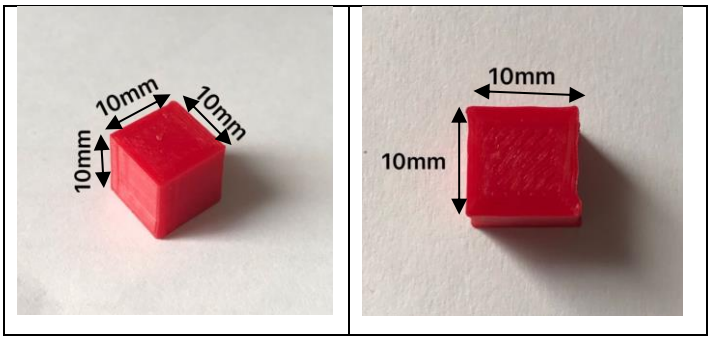

a) Isometric view *b) Top view*

Figure 4.1: 3D printed PLA sample with the dimension of (10mm x 10mm x 10mm) (WxLxH)

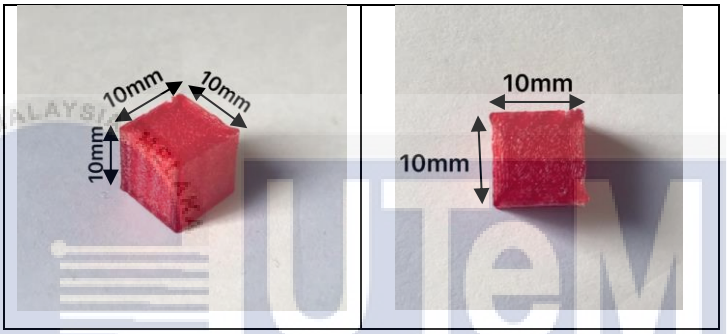

b) Isometric view *b) Top view*

Figure 4.2: 3D printed TPU sample with the dimension of (10mm x 10mm x 10mm) (WxLxH)

4.2 Fourier-Transform Infrared Spectroscopy (FTIR)

Fourier transform infrared spectroscopy (FTIR) is a technique for obtaining the infrared spectrum of solid, liquid, and gas absorption, emission, and photoconductivity. In this analysis, an FTIR machine was used to analyse polymeric chain bonding, particularly in the O-H group, to demonstrate the effect of moisture exposure on the filament.

4.2.1 Preparation of the FTIR Measurement

Figure 4.3: The employed FTIR, JASCO FT/IR 6100

Figure 4.4: All samples under a variety of conditions prepared to be analysed

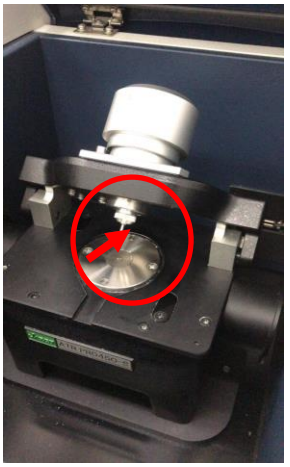

Figure 4.5: Measurement chamber and the auto sample presser

4.2.2 FTIR Analysis: PLA Specimens

Figure 4.6 shows the transmittance vs. wavelength graph obtained from the FTIR spectra analysis for the identification of the influence of water in the polymeric chemical chain bonding of the humidity exposed 3D printed PLA. The O-H bond is expected to be found in the range of wavenumbers from around 2800 cm^{-1} to 3000 cm^{-1}, as suggested by Olam and Tosun (2022). In this study, different chemical bonds of materials are analysed to investigate the influence of water on the polymeric chain of the thermoplastic polymers when the filaments are exposed to humidity, and the intensity of the transmittance is predicted to vary according to each condition.

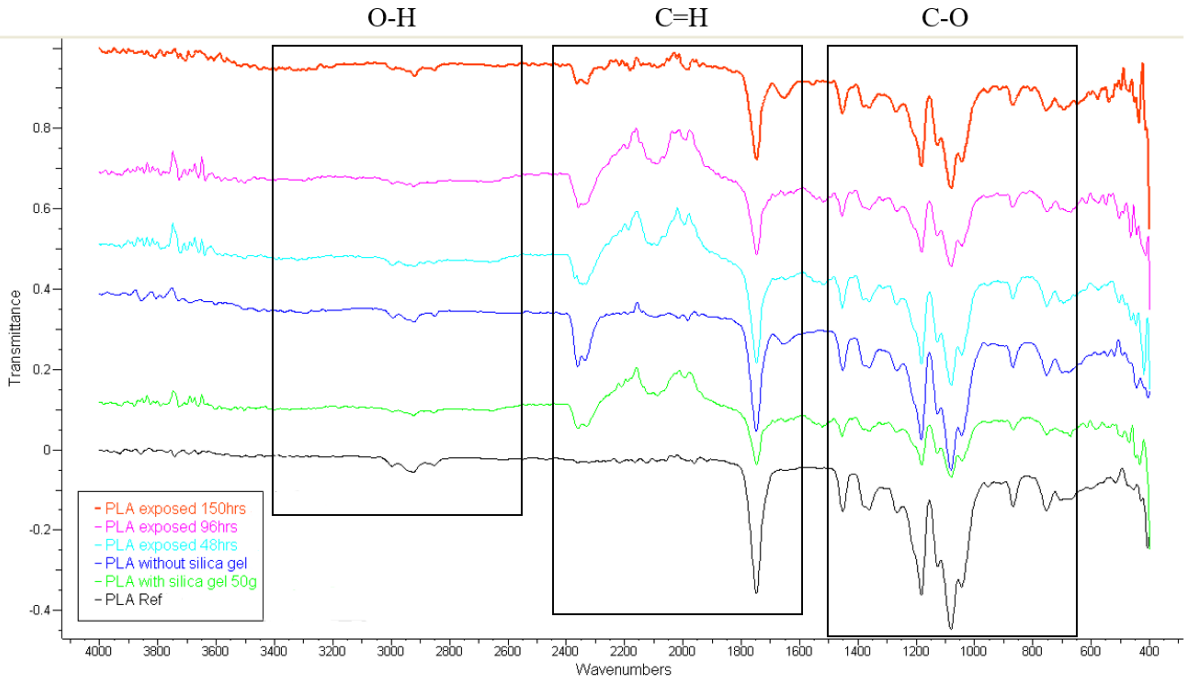

Figure 4.6: The difference intensity level of the hydrogen bonds (O-H) under different conditions for PLA specimen

Figure 4.6 depicts the chemical bonds found in the FTIR analysis. There are three different bonds in the graph, which are identified as hydroxide ion bond (O-H), carbon-hydrogen bond (C=H), and carbon monoxide bond (C-O). There are IR (Infrared Radiation) peaks or stretching bands that were analyzed on this graph according to the O-H region that has been marked. The O-H bond was spotted in the FTIR graph at a wavenumber range around 2800 cm^{-1} until 3000 cm^{-1}. The PLA specimens show the conditions as a reference filament starting at 0 transmittances and the exposed-moisture 150 hours is 1.0 transmittance.

From the graph illustrated in Figure 4.7, the highest peak O-H was spotted in conditions exposed by a humidifier for 150 hours, followed by 96 hours and 48 hours. Next, the conditions of PLA that were stored in a vacuum bag with silica gels portray a low intensity of the O-H bond compared to the PLA filament that was stored without any silica gels, which shows a slightly higher intensity of the O-H bond. This result indicates that the silica gels, or desiccants, effectively control the humidity if used during storage. As expected, the reference filament demonstrates the lowest intensity of the O-H bond. The results supported the findings from Pagnin et al. (2021) who suggested that the way a filament is exposed to moisture can affect the state of a polymeric chemical chain.

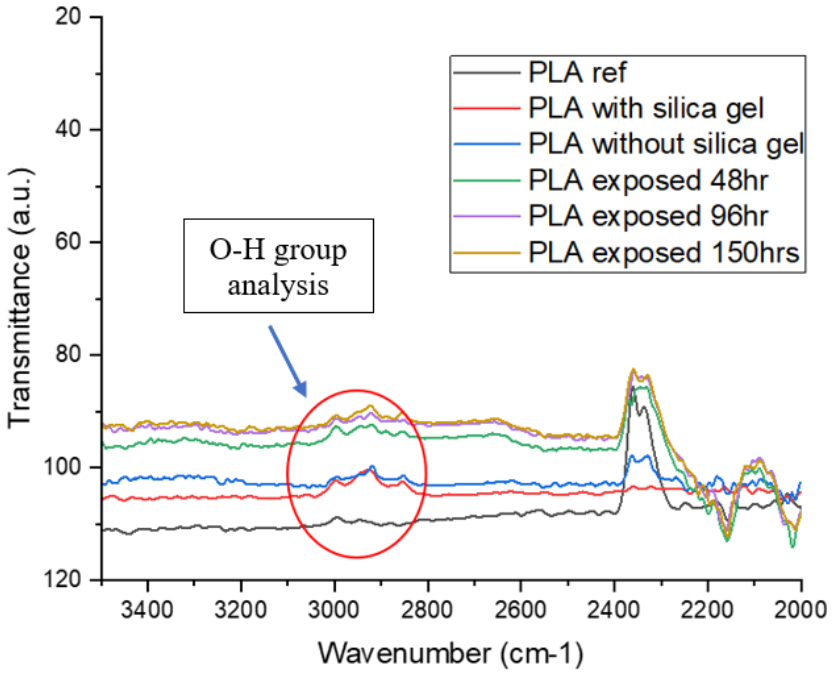

Figure 4.7: The transmittance vs. wavenumbers for different conditions of 3D printed PLA

4.2.3 FTIR Analysis: TPU Specimens

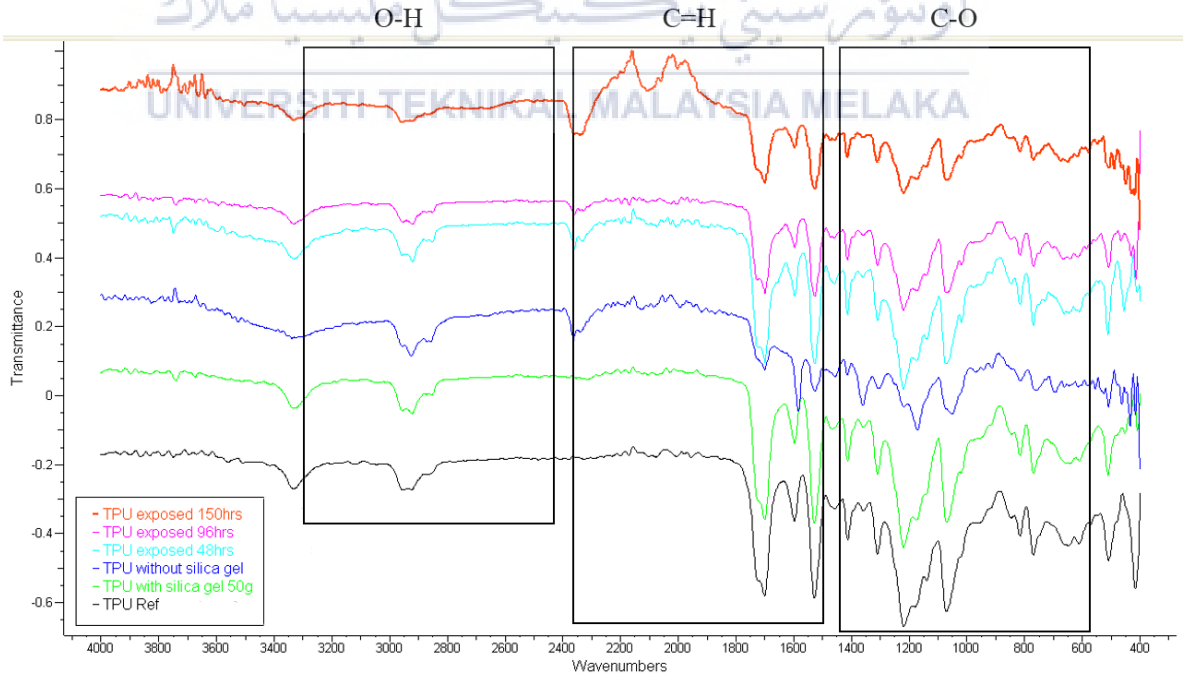

Figure 4.8: The difference intensity level of the hydrogen bonds (O-H) under different conditions for TPU specimens

The chemical bonds identified by the FTIR study are shown in Figure 4.8. The graph has three separate bonds: hydroxide ion bonds (O-H), carbon-hydrogen bonds (C=H), and carbon monoxide bonds (C-O). So, in this analysis, boxes of O-H marked with each chemical name were analysed. The conditions of TPU ref have a transmittance of -0.2, while the transmittance after 150 hours of exposure to moisture is 0.9 transmitted.

From the graph shown in Figure 4.9, the high-rise peak O-H was spotted in conditions exposed by a humidifier for 150 hours, followed by 96 hours and 48 hours. Following that, TPU stored in a vacuum bag containing silica gels exhibits a lower intensity of the O-H bond than TPU filament stored without silica gels, which exhibits a somewhat higher intensity of the O-H bond. This result indicates that the silica gels, or desiccants, effectively control the humidity if used during storage. As expected, the reference filament demonstrates the lowest intensity of the O-H bond.

The finding shows that the duration of humidity exposure (hours) proportionally contributes to the increase in transmittance for the O-H bond. The transmittance then shows a slight decrease in reading when the filament was stored in a vacuum bag without silica gel and in a vacuum bag with silica gel. The finding shows that, as a point of reference, the lowest peak is marked on a new filament TPU. We can conclude that the moisture effect will influence the water to polymeric chemical chain bonding. The water would make the graph become higher due to the variety of conditions for storage of the filaments. The humidity also makes the filament become worse and more quickly damaged. The differences in characteristics between PLA and TPU are not as great as with other filaments. Both filaments are popular in the 3D printing process but are also hydrophobic and easy to absorb humidity.

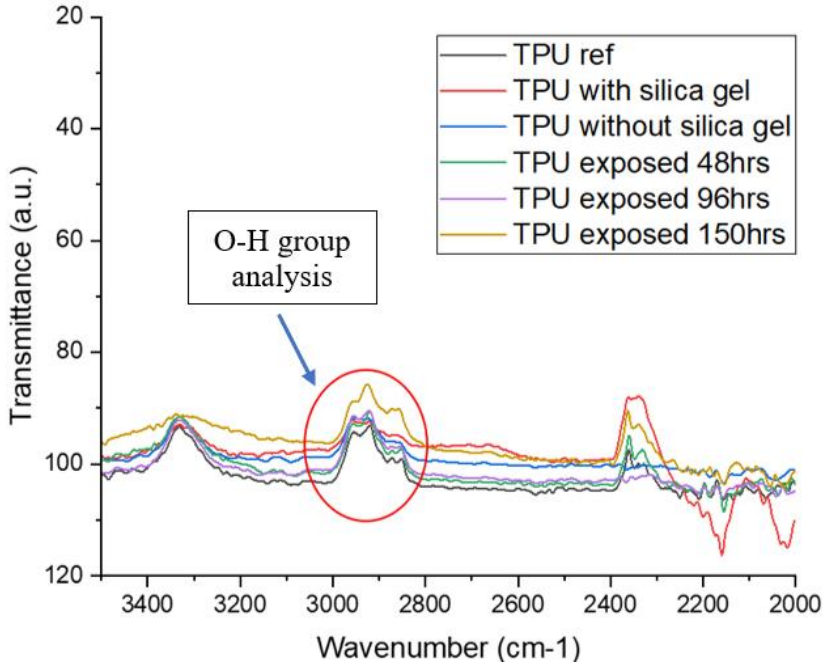

Figure 4.9: Transmittance vs. wavenumber A graph of the presence of hydrogen bonds in TPU 3D printed filaments

a)

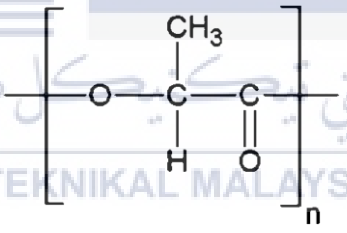

b)

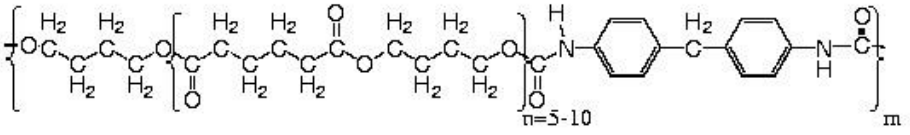

Figure 4.10: Chemical structure of a) PLA filament (Montané et al., 2020) and b) TPU filament (Kasprzyk et al., 2019)

As Figure 4.10 shows, the chemical structure between PLA and TPU filaments, and their chain bonding are different. TPU has a double bond and is longer than PLA, so its absorbance of humidity (H_2O) is faster (Deng et al., 2018).

Other than that, when polymers are broken down into smaller units that are called monomers, the molecule of water is used for each bond broken by these reactions, which are known as hydrolysis reactions. Water and polymers are naturally attracted to each other on account of both being polar molecules. Water will then react with the polymer in a process called hydrolysis. This will result in long polymer chains being cut down into shorter segments.

On a macro scale, shorter polymer chains mean that the filament becomes more brittle than flexible. When hydrolysis is allowed to proceed further, your filament may end up breaking apart into small pieces before you even get to feed it into a 3D printer. Unfortunately, hydrolysis cannot be reversed by just drying the filament after the effects have already set in (Zairullisham et al., 2021). All hydrolysis and dehydration reactions are similar for all macromolecules, but each monomer and polymer reaction is specific to its group.

Aside from that, the most important variables in the deterioration of plastic polymers are heat, light, air, and water. The most important chemical changes are oxidation and chain scission, which cause the molecular weight and degree of polymerization of the polymer to go down.

Analysed using Fourier Transform Infrared (FTIR) microspectroscopy in transmission mode to detect changes in the state of intermolecular hydrogen bonding as a function of 3D printed conditions. The FTIR transmittance bands associated with hydrogen bonding in 3D printed PLA under a variety of conditions have been identified, and the integrated molar absorption coefficients for the bands of interest have been determined experimentally.

4.3 Density Analysis of PLA-TPU Specimen using Archimedes Principle

The density test of the sample of 3D printed PLA-TPU was performed using a densimeter. The Archimedes Principle was applied in this test, which is the water immersion technique. According to science, the theoretical density of pure water has a density of 1 g/cm^3. Tables 4.1 – 4.2 tabulate the weight measurement in air and water at all conditions of PLA/TPU specimens, respectively.

Table 4.1: Density measurement of PLA specimen under all conditions

Type of conditions PLA		Weight in air (g)	Weight in water (g)	Density (g/cm^3)
New filament rolls as a reference		1.16	1.14	1.0354
Used filament roll stored in the vacuum bag with 50g desiccant/silica gel		1.19	1.16	1.0333
Used filament roll stored in the vacuum bag without desiccant/silica gel		1.17	1.16	1.0301
Exposed by humidified in various hours	48	1.17	1.15	1.0265
	96	1.16	1.15	1.0080
	150	1.17	1.15	1.0013

Figure 4.13 illustrates the density of all 3D printed PLA specimens under all conditions. The graph shows a continuous change in density measurement with a declining trend if the filament is exposed to humidity. The reference filament illustrates the maximum density, followed closely by the used filament stored in the vacuum bag with a 50g desiccant. The filament stored in a vacuum bag but without a desiccant has a slightly lower density than the one stored with silica gels. The density gradually dropped when the filament was exposed to a humidifier for 48 hours. Then, a steep decline in density was measured when the filament was exposed to humidity for 96 hours and continued to fall for 150 hours.

From this finding, it can be concluded that the exposure to humidity not only changes the material's chemical chain bonding, but the presence of water during printing can also affect the printed parts' porosity. Specimens that have been exposed to humidity show a low, dense measurement, which also indicates a high porosity in the microstructure. If the printed parts are porous, it will simultaneously affect the mechanical strength of the part. Therefore, due to the bad influence of humidity, the used filament must be kept in proper storage after use.

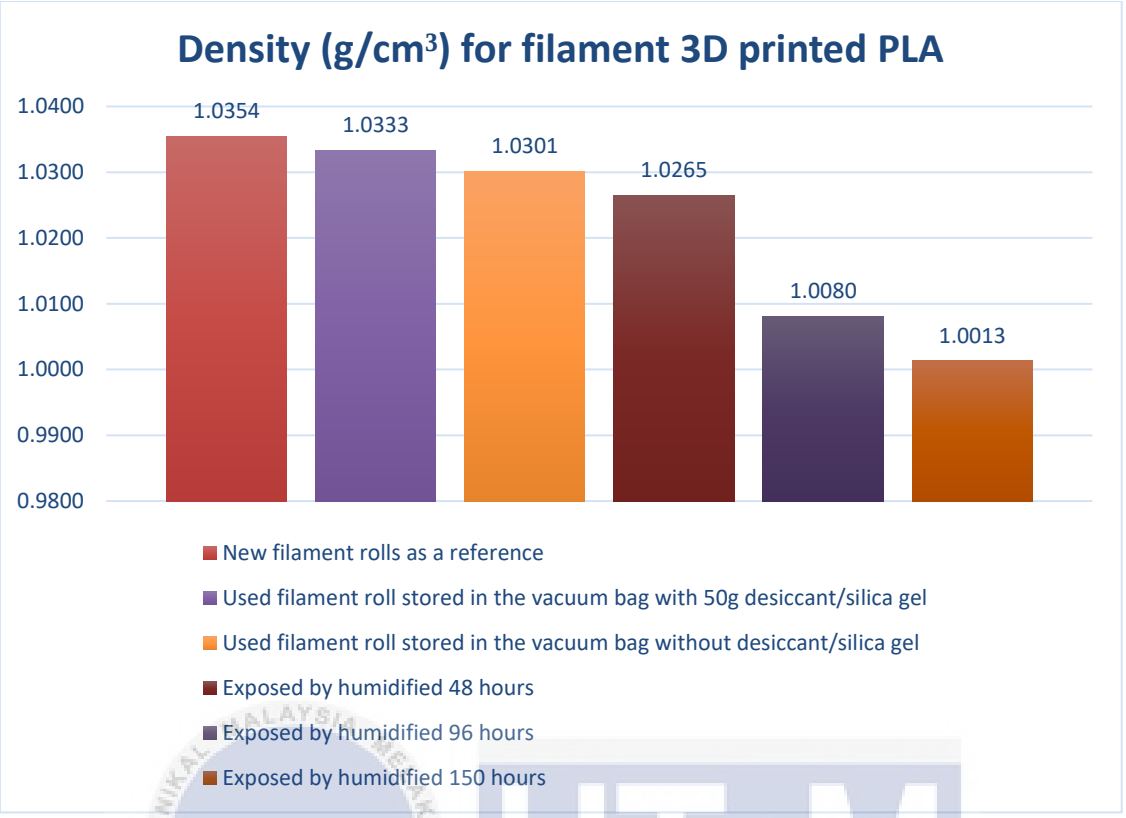

Figure 4.11: Density measurement of PLA specimen under different conditions

Table 4.2: Density measurement of TPU specimen under all conditions

Type of conditions TPU		Weight in air (g)	Weight in water (g)	Density (g/cm^3)
New filament rolls as a reference		0.93	0.90	0.8360
Used filament roll stored in the vacuum bag with 50g desiccant/silica gel		0.90	0.91	0.8270
Used filament roll stored in the vacuum bag without desiccant/silica gel		0.91	0.89	0.8250
Exposed by humidified in various of hours	48	0.93	0.86	0.8220
	96	0.93	0.91	0.8160
	150	0.89	0.87	0.8010

Figure 4.11 depicts the density of all 3D printed TPU specimens under all conditions. The graph shows a continuous change in density measurement with a declining trend if the filament is exposed to humidity. The reference filament illustrates the maximum density, followed closely by the used filament stored in the vacuum bag with a 50g desiccant. The density of the filament stored in a vacuum bag without a desiccant is slightly lower than that of the filament stored with silica gels. The density gradually dropped when the filament was exposed to a humidifier for 48 hours. After the filament had been exposed to humidity for 96 hours, a rapid reduction in density was seen that persisted for 150 hours exposed to humidity.

From this analysis, the difference between PLA and TPU is not as big as in other filaments, even though there are some differences in material inside both materials. However, the value of density was affected by the type of storage condition of the filaments. The filament that has a porous problem will not have a fully dense end after that. So, it's important to keep the filament in the best storage before the printing process.

Humidity makes the filament worse and will make the surface printed uneven. Therefore, due to the bad influence of humidity, the used filament must be kept in proper storage after use. Overall, we can see that the density is higher in the good condition storage of the filament of the TPU. This finding can conclude that the filament with the highest density has the fewest holes, while the filament with the lowest density has the most holes.

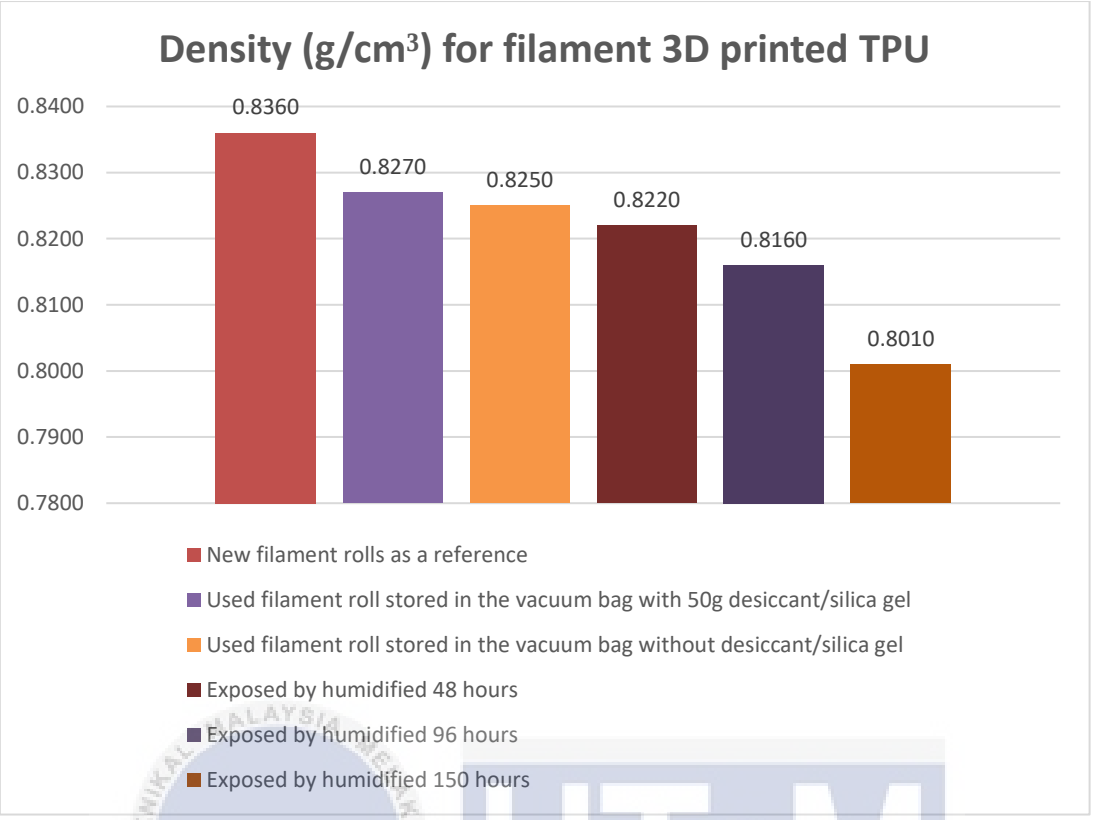

Figure 4.12: Density measurement of TPU specimen under different conditions

4.4 Microstructure Analysis (SEM)

The SEM analysis was conducted to observe the influence of humidity on the 3D printed part for different thermoplastic materials. PLA was chosen since it is the most used filament for 3D printer users. On the other hand, TPU was selected as different polymeric materials responded differently to the moisture in terms of the absorption rate. Therefore, a comparison of PLA and TPU was carried out in this analysis to see moisture's effect on their microstructure. As previously discussed, it has been mentioned that humidity decreases the material's density and increases the porosity. Therefore, in this SEM analysis, the porosity was observed under all conditions for both PLA and TPU specimens.

The purpose of SEM is to analyse the structural morphology of the 3D printed under the various conditions stated in this study. The list of conditions for 3D printed filament are: a) new filament roll PLA-TPU as a reference; b) used filament roll PLA-TPU stored in a

vacuum bag without silica gel; c) used filament roll PLA-TPU stored in a vacuum with silica gel; and the last condition is d) PLA-TPU exposed for 48, 96, and 150 hours using a humidifier in an open environment before the printing process.

Next, according to the flow chart of this study, microstructure analysis using an SEM machine is the last process of this study to identify the structural change of the humidity exposed 3D printed PLA-TPU. The unit was micrometer (µm), and the scale was fixed to 10µm, 200µm, and 300µm to be able to see the structural integrity of the 3D printed PLA-TPU. The electron magnification power used is 30x, 500x, and 1000x. From this analysis, there are 3 times the measurements at surface gap morphology than when the SEM image was taken, and the measurement is in horizontal shape for every condition of the surface of specimens. But for the limited amount of material sputter-coated at FKM Lab, there are only 4 conditions: specimens with 3 samples were coated using sputter coating.

4.4.1 Sputter Coating of Specimen

Before the process of SEM, it is necessary to sputter coat the surface of the sample with both 3D printed PLA and TPU filaments to remove the charging electrons from the material and obtain a good quality SEM image. All samples are sputter-coated with silver-palladium powder. Figure 4.13 shows the machine set up for the sputter coater and figure 4.14 shows the specimens that are being sputter coated.

Figure 4.13: The sputtering machine that was used to sputter the coating on the surface of the samples

Figure 4.14: The specimens after the process of sputter coating

4.4.2 SEM Analysis: PLA Specimen

Condition	SEM image	Discussion
Figure 4.15: Microstructure of PLA as a reference	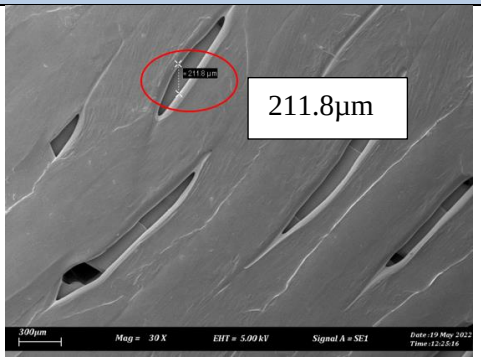	Figure 4.15 shows the lowest surface gap, which is 211.8µm, compared to Figure 4.16, which has 235.9µm.
Figure 4.16: Microstructure of PLA stored in the vacuum bag with silica gel	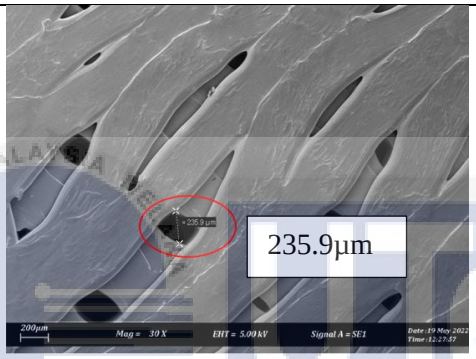	Figure 4.16 has 235.9µm of the surface gap and less than Figure 4.17 which has 273.8µm.
Figure 4.17: Microstructure of PLA stored in vacuum bag without silica gel	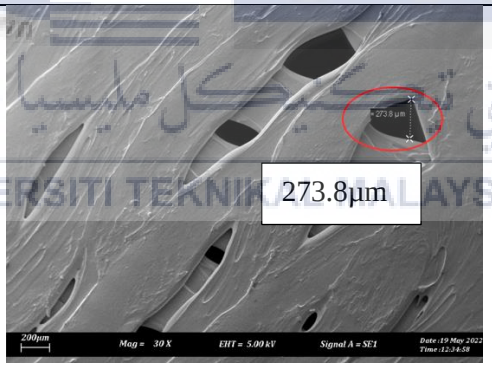	Figure 4.17 illustrates a 273.8µm surface gap than Figure 4.18 which is 296.5µm.
Figure 4.18: Microstructure PLA exposed for 150 hours by humidifier in an open environment	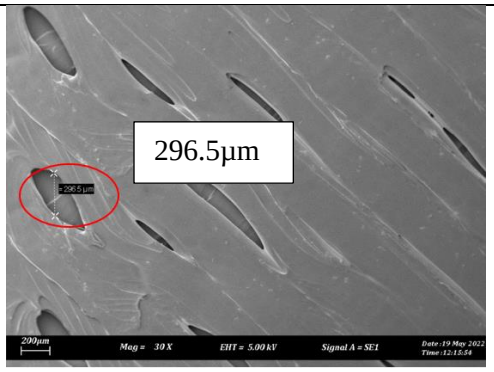	The highest surface gap is Figure 4.18 which has a length of 296.5µm.

Table 4.3: The length of structural of 3D printed PLA

Type of sample	Length 1	Length 2	Length 3	Average
	Micrometer (µm)			
New filaments roll PLA as a reference	211.80	216.90	220.90	216.53
Used filament roll PLA stored in the vacuum bag with silica gel	235.20	227.50	214.30	225.67
Used filament roll PLA stored in vacuum bag without silica gel	273.80	218.30	221.40	237.83
Exposed by humidified in 150 hours	296.50	280.10	257.30	277.97

Table 4.2 illustrates the length of the gap measured on the SEM images of the PLA specimen by measurement under the SEM image. The longest surface morphology gap shows the specimens using PLA filament that was exposed for 150 hours. The middle of the resultant surface gap is followed by conditions of filament roll PLA stored in a vacuum bag with silica gel, and finally, conditions of filament roll PLA stored in a vacuum bag without silica gel. The shortest surface morphology gap was spotted on the conditions of the new filament roll PLA as a reference.

4.4.3 SEM Analysis: TPU specimen

The differences image of the specimens in SEM image with 200x electron magnification power. From this analysis, there is 3 times the measurement at surface gap morphology under which the SEM image was taken, and the measurement is in horizontal shape for every condition of the surface of specimens. But for the limited amount of material sputter-coated at FKM Lab, there are only 4 conditions of TPU specimens with 3 samples coated using sputter coating. Structural changes are visible on each of the SEM images, although not large changes in length.

Condition	SEM image	Discussion
Figure 4.19: Microstructure of TPU as a reference	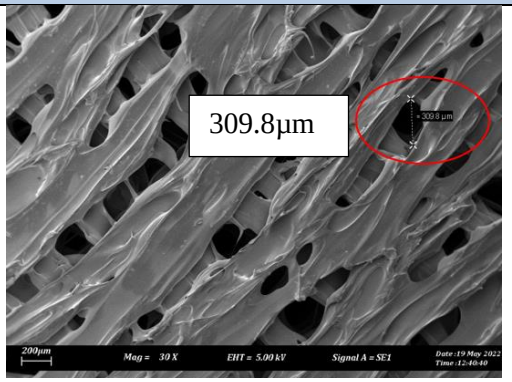	Figure 4.19 has a surface gap of 209.8µm, which is lower than Figure 4.20, which has 315.9µm.
Figure 4.20: Microstructure of TPU stored in the vacuum bag with silica gel	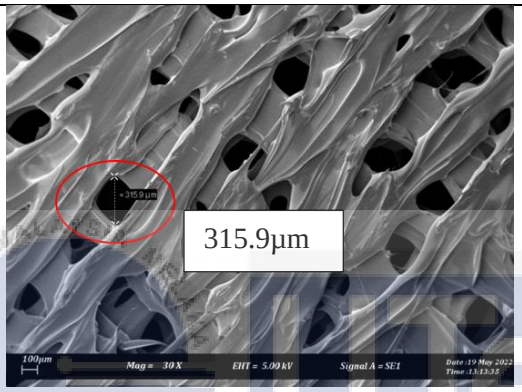	While Figure 4.20 has a surface gap of 315.9µm and the lowest of Figure 4.21 which has a length of 328.9µm.
Figure 4.21: Microstructure of TPU stored in vacuum bag without silica gel	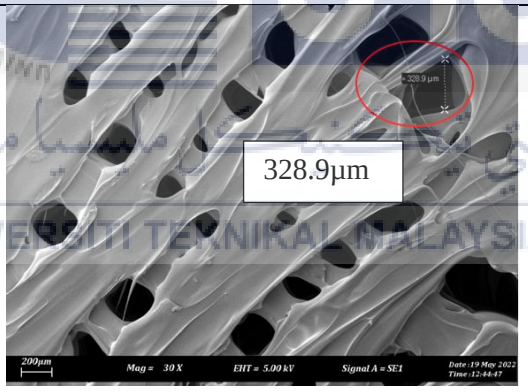	Next, Figure 4.21 has a surface gap of 328.9µm lower than condition Figure 4.22.
Figure 4.22: Microstructure TPU exposed for 150 hours by humidifier in an open environment	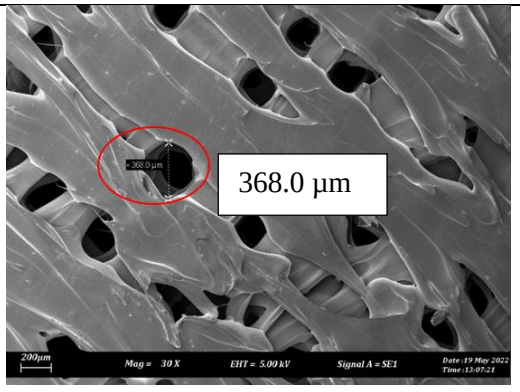	The exposed moisture in 150 hours in an open environment Figure 4.22 shows the highest surface gap based on all conditions which is 368.0 µm.

Table 4.4: The length of structural of 3D printed TPU

Type of sample	Length 1	Length 2	Length 3	Average
	Micrometer (µm)			
New filaments roll TPU as a reference	309.80	269.80	276.90	285.50
Used filament roll TPU stored in the vacuum bag with silica gel	315.90	279.31	288.20	294.47
Used filament TPU stored in vacuum bag without silica gel	328.90	281.20	299.80	303.30
Exposed by humidified in 150 hours	368.00	329.00	338.60	345.20

Table 4.4 indicates the length of the surface morphology gap in the SEM image of the 3D sample printed using TPU filament. The maximum surface morphology gap length was spotted in specimens with TPU filament that were exposed for 150 hours. The middle result of surface gap length is followed by specimens of filament roll TPU stored in a vacuum bag with silica gel, and then conditions of filament roll TPU stored in a vacuum bag without silica gel. The minimum surface morphology gap length is found in the specimen of a new filament roll TPU.

The humidity that was exposed to that filament has expanded the surface gap and affected the printing process. The structural change of each of the filaments is 3D printed according to the type of condition or storage of the filament before printing. Other than that, the microstructure analysis also shows the surface of prints the difference between those stored in good places and bad places. Therefore, this study concludes that the longer the surface morphology gaps, the higher the structural change of the humidity exposed on the 3D printed PLA-TPU filaments. The higher the structural change, the higher the porous of the filaments because of humidity. As the porosity of the specimen decreases, the density increases (Ayrilmis, 2018).

Many defects, such as cracks and gaps in 3D printed parts, adversely affect material properties. These imperfections have an important place in 3D printing parameters as well as the rheological properties of the material used. The morphological qualities of manufactured items deteriorate because of 3D printing parameters. Thermal strains are

created within the material because of the rapid heating and cooling cycle used in 3D printing. Deformations in the inner layer, cracks between adjacent layers, and raster orientation are all the result of these forces.

So, to avoid prolonged problems, it is important to take care of the 3D printed material before use to get 3D printing results that are in good condition. Next, plastic absorbs water more quickly than other materials, so keeping the plastic in the right way is one way to cut down on its exposure to moisture.

CHAPTER 5

CONCLUSION AND RECOMMENDATION

In this chapter, the conclusion for each objective of the study would be summarised, in addition to the recommendations for future studies.

5.1 Conclusion

This study investigated the influence of moisture on 3D printed PLA-TPU filament. The effect of humidity varied according to various conditions, and generally, the longer the filament was exposed to a humid environment, the more evident the influence would be. Adding any desiccant and sealing the filament in a vacuum environment reduced the exposure to humidity, highlighting the importance of storage conditions for the used filament. The following are the conclusions that can be drawn from this study for each specific objective study:

a) The first objective is to identify the influence of water absorption (H_2O) in the polymeric chemical chain bonding of the humidity-exposed 3D printed PLA-TPU filaments using Fourier Transform Infrared Spectroscopy (FTIR). For this objective, it was found that moisture changes the polymeric chemical bonding of the filament, and the hydrogen (O-H) bond was observed in the FTIR analysis. The intensity of the O-H bond varies steadily according to the set conditions. In conclusion, the longer the filament was exposed to the humidity, the more intense the O-H transmittance was recorded. Nevertheless, the control of the reference specimen indicates the lower intensity of the O-H bond, while the filament stored in a vacuum bag with desiccant

presented lower intensity of bond compared to the one stored without the desiccant. Also, TPU absorbs moisture faster than PLA, as the control specimen of TPU has recorded a -0.2 transmittance value as compared to the control specimen of PLA, with a nearly 0 value of transmittance.

b) As for the second objective concerning the porosity of the humidity-exposed 3D printed PLA-TPU filament under different humidity conditions using a densimeter. The more the filament was exposed to humidity, the less dense the 3D printed part became, indicating an increase in porosity. Nevertheless, the TPU specimen is more porous than PLA because it has a lower density. The filament that was stored in a vacuum bag with silica gel has a similar quality to the new filament, as a reference, which is the porous is lower than the exposed humidity of the other filament conditions.

c) As for the third objective, the structural change of the humidity-exposed 3D printed PLA-TPU filaments through microstructure analysis using SEM was successfully conducted. The microstructure analysis shows that the longer the surface morphology gaps, the higher the structural change of the humidity exposed on the 3D printed PLA-TPU filaments by following the measurement under SEM image. The higher the structural change, the higher the porous of the filaments because of humidity. Because of this, the SEM image of filament TPU shows more holes and pores than the SEM image of filament PLA.

However, the used PLA-TPU filament stored in a vacuum bag with some dehumidifying agents shows an equivalent result for FTIR to the reference specimens. In conclusion, humidity influences the 3D printed part under a variety of different conditions and should be controlled for good printing quality of PLA-TPU parts. This study is successful in improving the influence of the moisture due to the different conditions, and the result is to convey some messages to the user on the importance of keeping their used filament properly. At least this study shows the importance of avoiding humidity for 3D printing by using a standard way of keeping the filament. This research also aims to raise public awareness of the humidity issue, particularly regarding 3D printed materials.

5.2 Recommendation

In terms of future study, the following recommendations are suggested:

a) This study can be improved by using a proper humidity device such as a dry cabinet box with controllable humidity to control the humidity level.

b) PLA filaments should be stored in a drying cabinet with controllable humidity. If not, people who use 3D printers should put the used PLA filament in a vacuum bag with some dehumidifiers to keep it from getting moldy.

c) The humidity level in PLA filaments needs to be measured before printing to ensure good results. It is recommended to set up a real-time humidity measurement device during the 3D printing process to control the humidity factor.

d) Regular maintenance for the 3D printing machines and drying cabinets is needed to avoid defects. If there are many defective products produced, more plastic will end up in landfills, causing unsustainable 3D printing.

5.3 Sustainability

The material utilised in this study was biodegradable PLA-TPU filament. It is one of the most common materials that enable the economically practical manufacturing of nonpetroleum plastic. Ultimately, nature degrades when exposed to the environment. PLA is also one of the recyclable materials. Therefore, the printed PLA parts can be recycled through the correct procedure to ensure their sustainability. Aside from that, TPU is more eco-friendly than most other polymers. TPU is an innovative material that is considerably more environmentally friendly than alternatives such as PVC because it is recyclable and biodegradable in 3–5 years.

5.4 Lifelong Learning Element

Feature of lifelong learning is defined as a form of self-directed education that focuses on personal growth. Lifelong learning is also described as the formation of human capacity via a process that continually supports and promotes the acquisition of all the knowledge, values, abilities, and understanding necessary throughout life and can be applied to all the tasks. This study will help people learn more about the technology of additive manufacturing (AM).

5.5 Complexity Element

The 3D printing in the FKP lab was damaged and this made it difficult for us to get the specimens as quickly as possible. The filling will also cause the material to easily absorb moisture, so a little error may occur during this time. The humidity level was one of the study's complexities since it is difficult to control. Initially, the moisture meter was used to measure the humidity level in the filament, but it was unable to detect any measurement, despite the manufacturer's claim that it could be used to do so. Besides, the humidifier's water must be changed frequently because it only lasts for 2-3 hours. Due to the limited availability of laboratories during the COVID-19 pandemic epidemic, only the half conditions of the filaments were sputtered and were selected for microstructure examination using the scanning electron microscope (SEM).

REFERENCES

Algarni, M. (2021). *The Influence of Raster Angle and Moisture Content on the Mechanical Properties of PLA Parts Produced by Fused Deposition Modeling*. https://doi.org/10.3390/polym

Álvarez, S., Mullen, A. M., Hamill, R., O'Neill, E., & Álvarez, C. (2021). Dry-aging of beef as a tool to improve meat quality. Impact of processing conditions on the technical and organoleptic meat properties. *Advances in Food and Nutrition Research, 95*, 97–130. https://doi.org/10.1016/BS.AFNR.2020.10.001

Ameen, S. M., & Caruso, G. (2017). *Chemistry of Lactic Acid*. 7–17. https://doi.org/10.1007/978-3-319-58146-0_2

Amza, C. G., Zapciu, A., Constantin, G., Baciu, F., & Vasile, M. I. (2021). Enhancing mechanical properties of polymer 3D printed parts. *Polymers*, *13*(4), 1–18. https://doi.org/10.3390/polym13040562

Aurilia, M., Piscitelli, F., Sorrentino, L., Lavorgna, M., & Iannace, S. (2011). Detailed analysis of dynamic mechanical properties of TPU nanocomposite: The role of the interfaces. *European Polymer Journal*, *47*(5), 925–936. https://doi.org/10.1016/j.eurpolymj.2011.01.005

Ayrilmis, N. (2018). Effect of layer thickness on surface properties of 3D printed materials produced from wood flour/PLA filament. *Polymer Testing, 71*, 163–166. https://doi.org/10.1016/j.polymertesting.2018.09.009

Bacsik, Z., Mink, J., & Keresztury, G. (2004). FTIR spectroscopy of the atmosphere. I. Principles and methods. *Applied Spectroscopy Reviews, 39*(3), 295–363. https://doi.org/10.1081/ASR-200030192

Bellehumeur, C., Li, L., Sun, Q., & Gu, P. (2004). Modeling of bond formation between polymer filaments in the fused deposition modeling process. *Journal of*

Manufacturing Processes, *6*(2), 170–178. https://doi.org/10.1016/S1526-6125(04)70071-7

Bhandari, S., Lopez-Anido, R. A., & Gardner, D. J. (2019). Enhancing the interlayer tensile strength of 3D printed short carbon fiber reinforced PETG and PLA composites via annealing. *Additive Manufacturing*, *30*. https://doi.org/10.1016/j.addma.2019.100922

Cao, Y., Bolisetty, S., Wolfisberg, G., Adamcik, J., & Mezzenga, R. (2019). Amyloid fibril-directed synthesis of silica core–shell nanofilaments, gels, and aerogels. *Proceedings of the National Academy of Sciences of the United States of America*, *116*(10), 4012–4017. https://doi.org/10.1073/pnas.1819640116

Cubas-Cano, E., González-Fernández, C., Ballesteros, M., & Tomás-Pejó, E. (2018). Biotechnological advances in lactic acid production by lactic acid bacteria: lignocellulose as novel substrate. *Biofuels, Bioproducts and Biorefining*, *12*(2), 290–303. https://doi.org/10.1002/BBB.1852

Cui, Z. X., Shen, S., Wu, J. H., Si, J. H., Wang, Q. T., Turng, L. S., & Chen, W. Z. (2020). Functionalization of 3-d porous thermoplastic polyurethane scaffolds by two-stage polydopamine/hydroxyapatite composite nanoparticles. *Express Polymer Letters*, *14*(9), 794–807. https://doi.org/10.3144/expresspolymlett.2020.66

Deng, Y., Yu, C., Wongwiwattana, P., & Thomas, N. L. (2018). Optimising Ductility of Poly(Lactic Acid)/Poly(Butylene Adipate-co-Terephthalate) Blends Through Co-continuous Phase Morphology. *Journal of Polymers and the Environment*, *26*(9), 3802–3816. https://doi.org/10.1007/S10924-018-1256-X

Dey, A., & Yodo, N. (2019). A systematic survey of FDM process parameter optimization and their influence on part characteristics. In *Journal of Manufacturing and Materials Processing* (Vol. 3, Issue 3). MDPI Multidisciplinary Digital Publishing Institute. https://doi.org/10.3390/jmmp3030064

Elmrabet, N., & Siegkas, P. (2020). Dimensional considerations on the mechanical properties of 3D printed polymer parts. *Polymer Testing*, *90*.

https://doi.org/10.1016/j.polymertesting.2020.106656

Elvin, M. (n.d.). *The effect of humidity and temperature on paper properties*.

Fallon, J. J., Kolb, B. Q., Herwig, C. J., Foster, E. J., & Bortner, M. J. (2019). Mechanically adaptive thermoplastic polyurethane/cellulose nanocrystal composites: Process-driven structure–property relationships. *Journal of Applied Polymer Science*, *136*(4). https://doi.org/10.1002/app.46992

Frick, A., & Rochman, A. (2004). Characterization of TPU-elastomers by thermal analysis (DSC). *Polymer Testing*, *23*(4), 413–417. https://doi.org/10.1016/j.polymertesting.2003.09.013

Gupta, B., Revagade, N., & Hilborn, J. (2007). Poly(lactic acid) fiber: An overview. In *Progress in Polymer Science (Oxford)* (Vol. 32, Issue 4, pp. 455–482). https://doi.org/10.1016/j.progpolymsci.2007.01.005

Gussev, M. N., & Leonard, K. J. (2019). In situ SEM-EBSD analysis of plastic deformation mechanisms in neutron-irradiated austenitic steel. *Journal of Nuclear Materials*, *517*, 45–56. https://doi.org/10.1016/j.jnucmat.2019.01.034

Henton, D. E., Gruber, P., Lunt, J., & Randall, J. (2005). *Polylactic Acid Technology Acknowledgments Reference* (Issue 1).

Hossain, K. M. Z., Parsons, A. J., Rudd, C. D., Ahmed, I., & Thielemans, W. (2014). Mechanical, crystallisation and moisture absorption properties of melt drawn polylactic acid fibres. *European Polymer Journal*, *53*(1), 270–281. https://doi.org/10.1016/j.eurpolymj.2014.02.001

HUMIDITY ON FILAMENT - Google Search. (n.d.). Retrieved November 30, 2021, from https://www.google.com/search?q=HUMIDITY+ON+FILAMENT&sxsrf=AOaemvKx5TWV8WwofydFLCdLcpILEViEBg:1638268263061&tbm=isch&source=iu&ictx=1&fir=JOVNka7mqHtu6M%252Cum15PIwuFUxbMM%252C_&vet=1&usg=AI4_-kQU_EGZsECUfHpmxYz5Gj1LYRC7Gg&sa=X&ved=2ahUKEwi42_bu8L_0AhUsTmwGHSKrDT8Q9QF6BAgIEAE&biw=1920&bih=904&dpr=1#imgrc=Gxxi7F3Ft

BuRLM

Indrayanto, G., & Rohman, A. (2020). The Use of FTIR Spectroscopy Combined with Multivariate Analysis in Food Composition Analysis. *Spectroscopic Techniques & Artificial Intelligence for Food and Beverage Analysis*, 25–51. https://doi.org/10.1007/978-981-15-6495-6_2

Jamshidian, M., Tehrany, E. A., Imran, M., Jacquot, M., & Desobry, S. (2010). Poly-Lactic Acid: Production, applications, nanocomposites, and release studies. *Comprehensive Reviews in Food Science and Food Safety*, *9*(5), 552–571. https://doi.org/10.1111/J.1541-4337.2010.00126.X

Jantasee, S., Kienberger, M., Mungma, N., & Siebenhofer, M. (2017). Potential and assessment of lactic acid production and isolation – a review. *Journal of Chemical Technology and Biotechnology*, *92*(12), 2885–2893. https://doi.org/10.1002/JCTB.5237

Kakanuru, P., & Pochiraju, K. (2020). Moisture Ingress and Degradation of Additively Manufactured PLA, ABS and PLA/SiC Composite Parts. *Additive Manufacturing*, *36*. https://doi.org/10.1016/j.addma.2020.101529

Kasprzyk, P., Sadowska, E., & Datta, J. (2019). Investigation of Thermoplastic Polyurethanes Synthesized via Two Different Prepolymers. *Journal of Polymers and the Environment*, *27*(11), 2588–2599. https://doi.org/10.1007/S10924-019-01543-7

Kaszynka, M., Olczyk, N., Techman, M., Skibicki, S., Zielinski, A., Filipowicz, K., Wroblewski, T., & Hoffmann, M. (2019). Thermal-Humidity Parameters of 3D Printed Wall. *IOP Conference Series: Materials Science and Engineering*, *471*(8). https://doi.org/10.1088/1757-899X/471/8/082018

Klippstein, H., Diaz De Cerio Sanchez, A., Hassanin, H., Zweiri, Y., & Seneviratne, L. (2018). Fused Deposition Modeling for Unmanned Aerial Vehicles (UAVs): A Review. *Advanced Engineering Materials*, *20*(2). https://doi.org/10.1002/ADEM.201700552

Kong, L., Ostadhassan, M., Hou, X., Mann, M., & Li, C. (2019). Microstructure characteristics and fractal analysis of 3D-printed sandstone using micro-CT and SEM-EDS. *Journal of Petroleum Science and Engineering*, *175*, 1039–1048. https://doi.org/10.1016/j.petrol.2019.01.050

Lasprilla, A. J. R., Martinez, G. A. R., Lunelli, B. H., Jardini, A. L., & Filho, R. M. (2012). Poly-lactic acid synthesis for application in biomedical devices - A review. In *Biotechnology Advances* (Vol. 30, Issue 1, pp. 321–328). https://doi.org/10.1016/j.biotechadv.2011.06.019

Li, H., & Huneault, M. A. (2011). Effect of chain extension on the properties of PLA/TPS blends. *Journal of Applied Polymer Science*, *122*(1), 134–141. https://doi.org/10.1002/app.33981

Liao, Y., Liu, C., Coppola, B., Barra, G., di Maio, L., Incarnato, L., & Lafdi, K. (2019). Effect of porosity and crystallinity on 3D printed PLA properties. *Polymers*, *11*(9). https://doi.org/10.3390/polym11091487

Liu, W. K., Zhao, Y., Wang, R., Luo, F., Li, J. S., Li, J. H., & Tan, H. (2018). Effect of Chain Extender on Hydrogen Bond and Microphase Structure of Biodegradable Thermoplastic Polyurethanes. *Chinese Journal of Polymer Science (English Edition)*, *36*(4), 514–520. https://doi.org/10.1007/s10118-018-2020-3

Lv, C., Sun, X. C., Xia, H., Yu, Y. H., Wang, G., Cao, X. W., Li, S. X., Wang, Y. S., Chen, Q. D., Yu, Y. de, & Sun, H. B. (2018). Humidity-responsive actuation of programmable hydrogel microstructures based on 3D printing. *Sensors and Actuators, B: Chemical*, *259*, 736–744. https://doi.org/10.1016/j.snb.2017.12.053

Meng, X., Shi, G., Chen, W., Wu, C., Xin, Z., Han, T., & Shi, Y. (2015). Structure effect of phosphite on the chain extension in PLA. *Polymer Degradation and Stability*, *120*, 283–289. https://doi.org/10.1016/j.polymdegradstab.2015.07.019

Mitchell, M. K., & Hirt, D. E. (2015). Degradation of PLA fibers at elevated temperature

and humidity. *Polymer Engineering and Science*, *55*(7), 1652–1660. https://doi.org/10.1002/pen.24003

Mohamed, O. A., Masood, S. H., & Bhowmik, J. L. (2021). Modeling, analysis, and optimization of dimensional accuracy of FDM-fabricated parts using definitive screening design and deep learning feedforward artificial neural network. *Advances in Manufacturing*, *9*(1), 115–129. https://doi.org/10.1007/s40436-020-00336-9

Montané, X., Montornes, J. M., Nogalska, A., Olkiewicz, M., Giamberini, M., Garcia-Valls, R., Badia-Fabregat, M., Jubany, I., & Tylkowski, B. (2020). Synthesis and synthetic mechanism of Polylactic acid. *Physical Sciences Reviews*, *5*(12). https://doi.org/10.1515/PSR-2019-0102/HTML

Nazir, A., & Jeng, J. Y. (2020). A high-speed additive manufacturing approach for achieving high printing speed and accuracy. *Proceedings of the Institution of Mechanical Engineers, Part C: Journal of Mechanical Engineering Science*, *234*(14), 2741–2749. https://doi.org/10.1177/0954406219861664

Olam, M., & Tosun, N. (2022). 3D-printed polylactide/hydroxyapatite/titania composite filaments. *Materials Chemistry and Physics*, *276*, 125267. https://doi.org/10.1016/J.MATCHEMPHYS.2021.125267

Pagnin, L., Calvini, R., Wiesinger, R., & Schreiner, M. (2021). SO2- and NOx- initiated atmospheric degradation of polymeric films: Morphological and chemical changes, influence of relative humidity and inorganic pigments. *Microchemical Journal*, *164*. https://doi.org/10.1016/J.MICROC.2021.106087

Rajpurohit, S. R., & Dave, H. K. (2018). Effect of process parameters on tensile strength of FDM printed PLA part. *Rapid Prototyping Journal*, *24*(8), 1317–1324. https://doi.org/10.1108/RPJ-06-2017-0134

Rosi, F., Cartechini, L., Sali, D., & Miliani, C. (2019). Recent trends in the application of fourier transform infrared (FT-IR) spectroscopy in Heritage Science: From micro: From non-invasive FT-IR. *Physical Sciences Reviews*, *4*(11).

https://doi.org/10.1515/PSR-2018-0006/ASSET/GRAPHIC/J_PSR-2018-0006_FIG_011.JPG

Sanyang, M. L., Sapuan, S. M., Jawaid, M., Ishak, M. R., & Sahari, J. (2015). Effect of plasticizer type and concentration on tensile, thermal and barrier properties of biodegradable films based on sugar palm (Arenga pinnata) starch. *Polymers*, *7*(6), 1106–1124. https://doi.org/10.3390/polym7061106

Seng, C. T., A/l Eh Noum, S. Y., A/l Sivanesan, S. K., & Yu, L. J. (2020). Reduction of hygroscopicity of PLA filament for 3D printing by introducing nano silica as filler. *AIP Conference Proceedings*, *2233*. https://doi.org/10.1063/5.0001927

Shahmirzadi, M. R., Gholampour, A., Kashani, A., & Ngo, T. D. (2021). Shrinkage behavior of cementitious 3D printing materials: Effect of temperature and relative humidity. *Cement and Concrete Composites*, *124*. https://doi.org/10.1016/j.cemconcomp.2021.104238

Shahrubudin, N., Lee, T. C., & Ramlan, R. (2019). An overview on 3D printing technology: Technological, materials, and applications. *Procedia Manufacturing*, *35*, 1286–1296. https://doi.org/10.1016/j.promfg.2019.06.089

Slotwinski, J. A., & Garboczi, E. J. (2014). Porosity of additive manufacturing parts for process monitoring. *AIP Conference Proceedings*, *1581 33*, 1197–1204. https://doi.org/10.1063/1.4864957

Soares, J. B., Finamor, J., Silva, F. P., Roldo, L., & Cândido, L. H. (2018). Analysis of the influence of polylactic acid (PLA) colour on FDM 3D printing temperature and part finishing. *Rapid Prototyping Journal*, *24*(8), 1305–1316. https://doi.org/10.1108/RPJ-09-2017-0177

Valerga, A. P., Batista, M., Salguero, J., & Girot, F. (2018). Influence of PLA filament conditions on characteristics of FDM parts. *Materials*, *11*(8). https://doi.org/10.3390/ma11081322

Veerasingam, S., Ranjani, M., Venkatachalapathy, R., Bagaev, A., Mukhanov, V., Litvinyuk, D., Mugilarasan, M., Gurumoorthi, K., Guganathan, L., Aboobacker, V. M., & Vethamony, P. (2021). Contributions of Fourier transform infrared spectroscopy in microplastic pollution research: A review. *Critical Reviews in Environmental Science and Technology*, *51*(22), 2681–2743. https://doi.org/10.1080/10643389.2020.1807450

Wang, L., Cavaco-Paulo, A., Xu, B., & Martins, M. (2018). Humidity induces changes in the dimensions of hydrogel-coated wool yarns. *Polymers*, *10*(3). https://doi.org/10.3390/polym10030260

Wasti, S., & Adhikari, S. (2020). Use of Biomaterials for 3D Printing by Fused Deposition Modeling Technique: A Review. *Frontiers in Chemistry*, *8*. https://doi.org/10.3389/FCHEM.2020.00315/FULL

Wei, Q., Li, H., Liu, G., He, Y., Wang, Y., Tan, Y. E., Wang, D., Peng, X., Yang, G., & Tsubaki, N. (2020). Metal 3D printing technology for functional integration of catalytic system. *Nature Communications*, *11*(1). https://doi.org/10.1038/s41467-020-17941-8

Woern, A. L., Byard, D. J., Oakley, R. B., Fiedler, M. J., Snabes, S. L., & Pearce, J. M. (2018). Fused particle fabrication 3-D printing: Recycled materials' optimization and mechanical properties. *Materials*, *11*(8). https://doi.org/10.3390/ma11081413

Xu, W., Jambhulkar, S., Zhu, Y., Ravichandran, D., Kakarla, M., Vernon, B., Lott, D. G., Cornella, J. L., Shefi, O., Miquelard-Garnier, G., Yang, Y., & Song, K. (2021). 3D printing for polymer/particle-based processing: A review. In *Composites Part B: Engineering* (Vol. 223). Elsevier Ltd. https://doi.org/10.1016/j.compositesb.2021.109102

Zahid, M., del Río Castillo, A. E., Thorat, S. B., Panda, J. K., Bonaccorso, F., & Athanassiou, A. (2020). Graphene morphology effect on the gas barrier, mechanical and thermal properties of thermoplastic polyurethane. *Composites Science and Technology*, *200*. https://doi.org/10.1016/j.compscitech.2020.108461

Zaldivar, R. J., Mclouth, T. D., Ferrelli, G. L., Patel, D. N., Hopkins, A. R., & Witkin, D. (2018). Effect of initial filament moisture content on the microstructure and mechanical performance of ULTEM ® 9085 3D printed parts. *Additive Manufacturing*, *24*, 457–466. https://doi.org/10.1016/j.addma.2018.10.022

Zhang, P., Wang, Z., Li, J., Li, X., & Cheng, L. (2020). From materials to devices using fused deposition modeling: A state-of-art review. *Nanotechnology Reviews*, *9*(1), 1594–1609. https://doi.org/10.1515/NTREV-2020-0101/ASSET/GRAPHIC/J_NTREV-2020-0101_FIG_003.JPG

APPENDICES

A Gantt Chart of PSM 1

No	Task	Semester 1 (Week)															
		1	2	3	4	5	6	7	8	9	10	11	12	13	14	15	16
1	PSM Title Registration								Mid-Semester Break							Study Week	Final Exam
2	Briefing of Title Selection																
3	Find Journals and Reference Materials on the PSM Title																
4	Define Objectives and Problem Statement																
5	Identify Background and Scope of Study																
6	Carry Out for Literature Review																
7	Conduct on Findings Methodology of Overall Process, Methods, and Instruments																
8	Submission of Logbook to Supervisor																
9	Preparation of Presentation PSM																
10	Presentation for PSM on Online Video																
11	Final Report PSM Checked by Supervisor																
12	Submission of PSM Report to Supervisor and Examiner																

	Plan
	Mid-Semester Break, Study Week, and Final Exam

B Gantt Chart of PSM 2

No	Task	Week															
		Semester 2 (February-July)															
		1	2	3	4	5	6	7	8	9	10	11	12	13	14	15	16	17
1	PSM Planning								Mid-Semester Break							Study Week	Final Exam	
2	Preparation for Laboratory																	
3	Discussion with Supervisor for Project Operation																	
4	Exposes to the moisture content and 3D printing process																	
5	FTIR Analysis, Density test and SEM Analysis																	
6	FTIR Analysis, Density test and SEM Analysis																	
7	Analyses Data from Testing Result																	
8	Submission of Logbook to Supervisor																	
9	Preparation of Presentation PSM																	
10	Presentation for PSM on Online Video																	
11	Final Report PSM Checked by Supervisor																	
12	Submission of PSM Report to Supervisor and Examiner																	

	Plan
	Mid-Semester Break, Study Week, and Final Exam